TAMPEREEN TEKNILLINEN YLIOPISTO
TAMPERE UNIVERSITY OF TECHNOLOGY

ELIZAVETA CHERVYACHKOVA

SYNTHETIC POLY(ETHYLENE GLYCOL)-BASED HYDROGEL PLATFORM FOR IN VITRO CELL STUDIES IN 3 DIMENSIONS

Master of Science Thesis

Examiner: Professor Minna Kellomäki

Examiner and topic approved by the Council of the Faculty of Natural Sciences on 8 November 2013

ABSTRACT

TAMPERE UNIVERSITY OF TECHNOLOGY
Master's Degree Programme in Biomedical Engineering
CHERVYACHKOVA, ELIZAVETA: Synthetic poly(ethylene glycol)-based hydrogel platform for in vitro cell studies in 3 dimensions
Master of Science Thesis, 51 pages
June 2014
Major: Biomaterials
Examiner: Professor Minna Kellomäki
Keywords: extracellular matrix, hydrogel, mechanical properties, PEG, Michael-addition reaction, vinyl sulfone, maleimide, mesh size, cell encapsulation

The behavior of cells cultured in two-dimensions (2D) greatly differs from that in three-dimensions (3D), and often does not reflect the actual *in vivo* situation. Consequently, 3D model systems are becoming more widely used as a tool for *in vitro* cell research. Hydrogels are polymer networks that contain large amounts of water and are potentially biocompatible. Therefore, hydrogels that mimic natural extracellular matrix (ECM) are being developed as 3D platforms for *in vitro* cell studies. Poly(ethylene glycol)-based (PEG) hydrogels are artificial gels that allow control over biophysical and biochemical parameters. Moreover, PEG hydrogels are known to be generally not cytotoxic which makes them widely used in a variety of biomedical applications.

This thesis has two major parts. The first part is the synthesis and characterization of PEG-based hydrogels via utilizing Michael-type addition reaction of unsaturated double bonds to thiols. Characterization included observation of elastic properties using atomic force microscopy (AFM) and performing swelling study from which the theoretical mesh sizes of hydrogels were calculated. The actual mesh sizes were checked via beads incorporation into the hydrogels' network. Moreover, the ranges, within which gels are reproducibly forming, were obtained for a variety of hydrogels and the gelation kinetics was checked using the oscillatory rheology. The second part of this thesis deals with the cell encapsulation into the hydrogel network and observation of cell viability. LS174T cell line was encapsulated into the PEG vinyl sulfone hydrogel with cleavable matrix metalloproteinase peptide (cMMP).

The results of the hydrogel development and characterization part have shown that it is possible to controllably modify mechanical properties of PEG hydrogels. Change of the PEG concentration and incorporation of linear PEGs in between the tetrafunctional ones has proven to have a impact on the mechanical properties of the gels.

The results of cell encapsulation part have shown that it is possible to encapsulate LS174T cell line in the kind of hydrogels that was developed and evaluated in this project. However, it remains a matter of future work to optimize the setting and meet the challenges regarding the reproducibility of these experiments and viability of encapsulated cells.

PREFACE

This Master of Science thesis has been conducted at the Max Planck Institute for Intelligent Systems, Stuttgart, in collaboration with Physical Chemistry Institute, Heidelberg University.

First of all, I would like to express my sincere gratitude to my supervisor Dr. Dimitris Missirlis for giving me the opportunity to work on such an interesting and challenging project and for providing me necessary guidance and support whenever needed. Thanks for your valuable instructions and comments and for all the time you have spent on this project. I am also grateful to the whole Spatz group for having an opportunity to work in such a good environment.

Furthermore, I want to thank my dear parents, Anna Shashmurina and Sergei Chervyachkov, for the love and care they have provided to me. Thank you for all the help and support along my life.

I would also like to give a special thanks to my friends, Varvara Sharova, Cynthia Frommelt, Aleksandra Shakun and all the others who were supporting and encouraging me. The time spent with you was great and unforgettable.

Finally, I would like to thank my boyfriend, Maximilian Ziebell, for always being so loving and supportive throughout the course of this work, and for motivating me to keep trying to improve. Thank you for your patience and always having time for me whenever needed.

Heidelberg, June 2014

Elizaveta Chervyachkova

ABBREVIATIONS

2D	–	Two-dimensional
3D	–	Three-dimensional
AFM	–	Atomic Force Microscopy
APTES	–	(3-Aminopropyl)triethoxysilane
cMMP	–	Cleavable Matrix Metalloproteinase peptide
EDTA	–	Ethylenediaminetetraacetic acid tetrasodium salt dehydrate
DTT	–	Dithiothreitol
EMEM	–	Eagle's Minimum Essential Medium
ECM	–	Extracellular Matrix
FBS	–	Fetal Bovine Serum
MW	–	Molecular Weight
PBS	–	Dulbecco’s Phosphate Buffered Saline
PEG	–	Poly(ethylene glycol)
Pen/Strep	–	Penicillin/streptomycin
VS	–	Vinyl Sulfone

CONTENTS

1. Introduction

1.1. Motivation

In order to study and understand basic cellular functions, scientists have been isolating cells from tissues and studying their function in vitro. At present, the majority of in vitro experimentation is performed on rigid, flat surfaces that do not efficiently capture important physical parameters (e.g. elasticity, confinement) present in vivo. Model three dimensional systems that are mimicking the extracellular matrix (ECM) could provide a more physiological setting for in vitro cell research, such as cell migration studies.

1.2. Approach

In this project, poly(ethylene glycol)-based (PEG) hydrogels were developed as a platform for in vitro cell studies. It is possible to form such hydrogels via cross-linking of PEG precursors utilizing mild and cytocompatible chemistry, namely the Michael-type addition of unsaturated double bonds to thiols. Through mixing of several designed components, the network architecture and therefore the mechanical properties of the hydrogels can be controlled. Moreover, one of the components was engineered to be responsive to cell-secreted proteases, so that the cells can actively cleave the network structure and make space for their growth and proliferation.

Encapsulation of cells in these hydrogels was achieved by simply mixing the polymer precursors with cells; gelation therefore occurred around the cell, leading to its entrapment in the polymer network. Cell-adhesive peptides could be incorporated in the network in order to allow cells to attach and exert traction forces, which are vital for the functions. It was previously shown that the proliferation and cell migration depend on the architecture and properties of the hydrogel [7, 18, 39, 40].

1.3. Objectives of the project

The overall objective of this project was to develop and evaluate an elastic, polymeric material that allows encapsulation and proliferation of live cells in a more physiological three-dimensional setting. In particular, the establishment of the preparation procedure of hydrogels with controlled mechanical properties was the main goal.

The project consisted of two main parts. In the first part of the project the conditions for gel formation and control of gel properties were determined. The gels were characterized in respect to viscoelasticity by oscillatory rheology, atomic force microscopy (AFM) and swelling measurements. Through the use of appropriate models, the theoretical pore sizes of the gels were also calculated. The second part of the project concentrated on the optimization of the cell encapsulation process. Cell survival and growth were quantified and correlated with the properties of the hydrogels.

2. Theoretical background

2.1. Three-dimensional platforms for cell-ECM interactions

2.1.1. Extracellular Matrix

The extracellular matrix (ECM) is the non-cellular component, which is present within all tissues and organs. It provides the essential physical scaffolding for the cells as well as crucial biochemical and biomechanical signals that are required for organ function (i.e. morphogenesis, differentiation, homeostasis and regeneration after damage). [1]

Essentially, the ECM is composed of various protein fibers interwoven within a highly hydrated network of polysaccharide chains. The exact ECM composition and architecture is tissue-specific as well as notably heterogeneous. The anisotropic fibrillar architecture of natural ECMs has an influence on cell behavior. Cells use cell-surface receptors (such as integrins, discoidin domain receptors and syndecans) to link their cytoskeleton to the ECM. Moreover, cells are able to transduce mechanical signals into biochemical signals (by binding growth factors (GFs) cells sense and respond to the mechanical properties of their environment by converting mechanical signals into chemical signals). Consequently, ECM directs essential tissue morphological organization and physiological function of cells within these tissues, which are critical for cell proliferation and migration. Moreover, structural ECM features, such as fibril shape and pore size distribution, often greatly influence cellular processes involved in migration, thereby dictating the strategy by which cells migrate through ECMs. Furthermore, the ECM is a highly dynamic structure which undergoes constant remodeling, either enzymatically or non-enzymatically. In some pathological situations, such as cancer (notably breast cancer), the structure of ECM may change significantly. [1, 2]

2.1.2. Mechanisms of cell migration in 3D matrixes

Cell migration is an essential process in development, immune surveillance and wound healing, among others. Cells use different mechanisms in order to migrate within the ECM. Two main modes of cell migration in 3D are: 1) proteolytic migration (also called mesenchymal migration), and (2) non-proteolytic migration (also called amoeboid). [5, 7]

Mesenchymal cell migration (Figure 2.1 A) is typically characterized by the following coordinated steps: exploration by the leading edge, formation of new adhesions, maturation of adhesions, advancement of the cell body over these adhesions, and release of adhesions to pull the rear forward. The cells that are wider than the matrix pore size

degrade the matrix via proteolytic and force-based matrix remodeling, thus migrating in a ‘‘path-generating’’ manner. Besides the structural coupling of the cytoskeleton with the ECM, cell-ECM adhesions can also facilitate the local expression of various proteases that are able to degrade neighboring ECM and basement membrane components and remove barriers allowing for cell translocation. The most studied proteases that cells use for this purpose belong to the metalloproteinase family. Both secreted and membrane type matrix metalloproteinases (MMPs) have been reported to affect normal and cancer cell migration. [5, 6, 7]

The second main mode of migration is amoeboid migration (Figure 2.1 B). It is characterized by an ellipsoid cell shape, formation of bleb-like protrusions, restriction of actomyosin contractility to the cell cortex and transient, dynamic adhesions with the ECM. The amoeboid cells squeeze through the preexisting pores in a protease-independent fashion, thus migrating in a ‘‘path-finding’’ manner. [7]

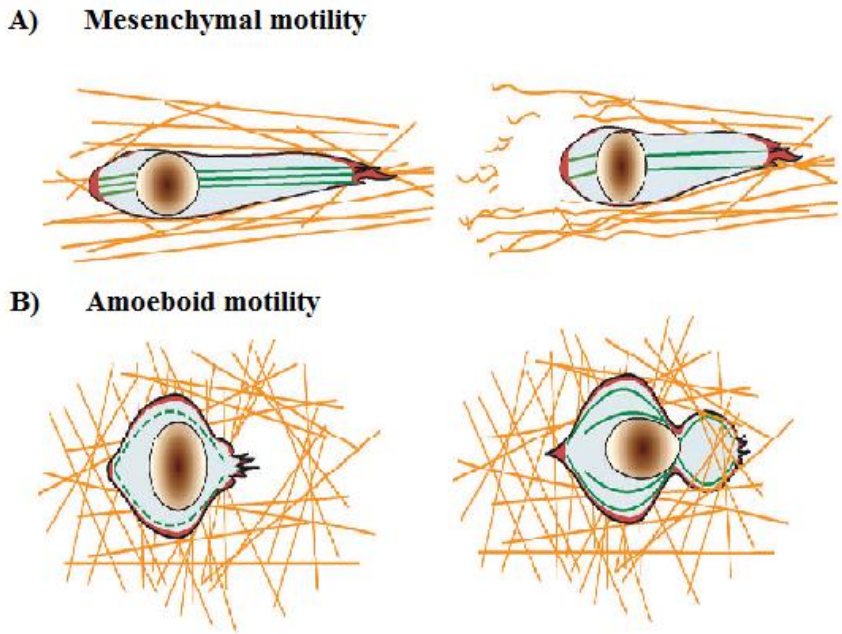

Figure 2.1. A) Mesenchymal mode of motility with elongated spindle-shaped morphology, focal adhesions at the poles, enhanced stress fiber contractility and proteolytic and force-based matrix remodeling; B) Amoeboid mode of motility with blebby protrusions, rounded ellipsoid morphology and cortical contractility. [7]

2.1.3. Naturally derived ECM

It has long been realized that in order to study and understand cell behavior, there is a need to study cells within the context of a specific microenvironment. The model systems developed allow to mimic the in vivo situation to a certain degree as well as to reduce the complexity. Two-dimensional in vitro models are widely used in

cell studies; however, it is undoubted that three-dimensional matrixes are more physiological. [2]

There is a wide range of naturally derived ECM 3D matrices used nowadays. Generally, naturally derived materials are purified protein components from animal tissues, e.g. collagen, or commercially available Matrigel, a solubilized basement membrane extract from mouse tumors. They are advantageous due to their ECM-like properties and biological recognition. However, they are limited by poor design flexibility, handling characteristics, purification difficulties, as well as batch-to-batch composition differences that affect the reproducibility of the experimental outcomes. Therefore, biomaterial scientists and tissue engineers have additionally explored the development of synthetic hydrogel platforms that mimic the essential features of ECM and that are biochemically and biophysically flexible. [2, 3]

2.1.4. Synthetic hydrogels

Hydrogels are highly hydrophilic polymer networks that contain large amounts of water. Since they were developed in the 1960's, hydrogels have been of great interest to biomedical scientists due to their potential biocompatibility and high water content, which resembles many tissue matrices [4, 8, 10].

Poly(ethylene glycol) (PEG) is a neutral polyether that is soluble in water and most organic solvents. PEG can be linear or branched, and it is available in a variety of molecular weights. PEG is generally nontoxic to cells and therefore it has found many applications in biotechnology and materials science, including preparation of PEG hydrogels; these can be synthesized via covalent cross-linking of PEG precursors with reactive end-functional groups. PEG hydrogels are hydrophilic, have neutral charge and are typically biocompatible. Their inert, protein-repellent character prevents non-specific cell adhesion, allowing selective functionalization with desired ligands. For example, through co-polymerization of ligands it is possible to introduce different functional moieties to suppress or promote cell survival and function. [8, 9, 11]

Generally, there are three possible cross-linking reaction mechanisms: chain-growth, step-growth, and mixed-mode chain and step growth (Figure 2.2). The main disadvantage of chain-growth polymerization, comparing to the step-growth, is that it can lead to lower conversion of the functional groups. Therefore, there are certain network non-idealities such as un-reacted monomers and/or functional groups that may affect the material properties and lower cell survival. [11]

In contrast to the chain growth mechanism, step-growth gelation occurs when at least two multifunctional monomers with mutually reactive chemical groups are reacted together in either stoichiometric balanced or imbalanced ratio, and the average monomer functionality is greater than 2 (Figure 2.2). This approach produces fewer structural defects during network formation and allows more precise control over the gel cross-linking density and subsequent material properties. It is possible to form degradable hydrogels via step-growth Michael-type addition reaction between vinyl sulfone func-

tionalized multi-arm PEG polymer and cleavable dithiols which was shown in previous studies [12]. This reaction decreases possible cell damage due to propagating free radicals as occurred in chain-growth polymerization and, therefore, is appropriate for *in vitro* encapsulation studies in hydrogels. [11, 12]

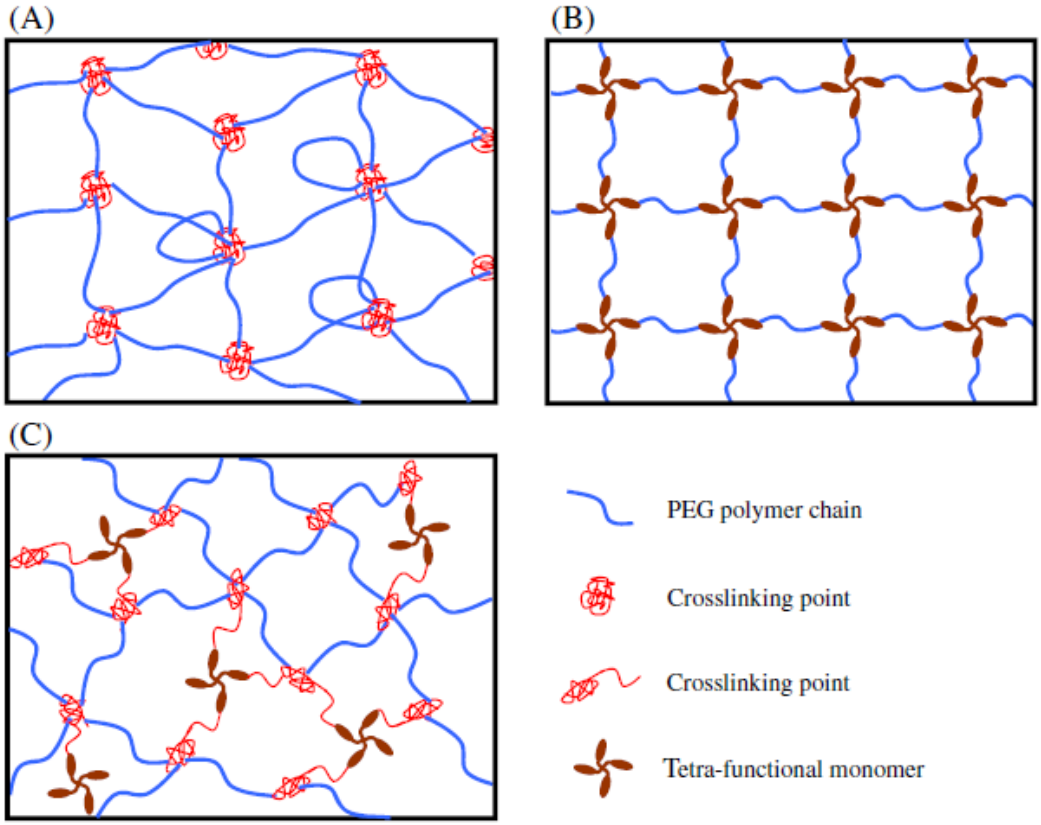

Figure 2.2. Schematic structures of PEG hydrogels formed via: A) chain-growth; B) step growth; and C) mixed-mode step and chain growth polymerization. [modified from 11]

2.2. Characterization techniques

When designing a hydrogel platform for *in vitro* applications it is essential that the developed matrix system maintains its physical and mechanical properties. There is a range of characterization techniques that can be applied in order to determine these properties. Below the techniques that were used in this project are described.

2.2.1. Atomic Force Microscopy

The Atomic Force Microscope (AFM) is widely known as a high-resolution imaging tool. However, the AFM is also a useful tool for sensitive force measurements and

can be used to determine mechanical properties of materials, such as their elastic modulus.

In the "Force Spectroscopy" mode the cantilever is moved towards the sample with the use of a piezo-electrically sensitive motor until the cantilever comes into contact with it. If the sample is rigid, further movement of the stage results in a corresponding deflection of the cantilever. On the other hand, if the sample is deformable, the cantilever additionally indents into the sample as a function of the mechanical properties of both the cantilever and the sample. The cantilever is then retracted while its deflection is being constantly measured. The schematic diagram of the cantilever-tip movement during a typical measurement is shown in the Figure 2.3A. If the sum of forces is attractive when the cantilever comes close to the surface, the tip may jump into the contact with the surface ("snap-in") (Figure 2.3B). Once the cantilever is in contact with the surface, it may be pushed into the sample with some force allowing the mechanical properties to be measured. [16]

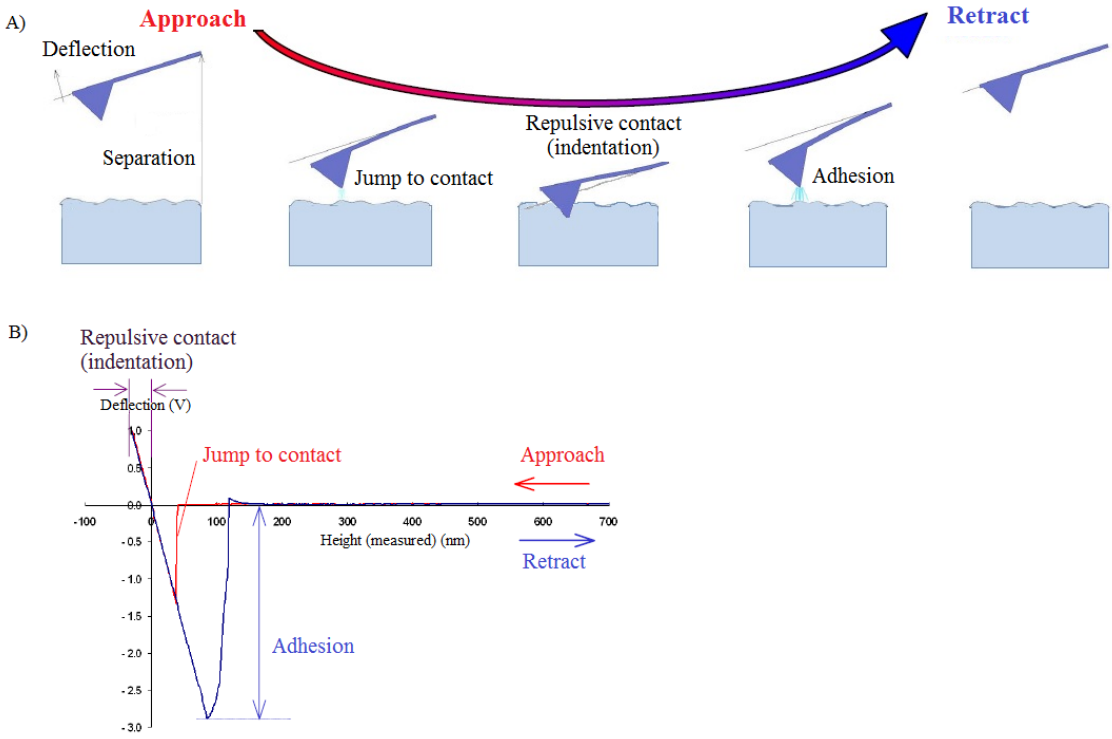

Figure 2.3. A) Schematic diagram of the vertical tip movement during approaching and retraction; B) A graph of a model measurement showing the different stages: approach, contact, repulsive contact (indentation), and retraction. [modified from 16]

The measurement consists of relating the deflection of the cantilever spring to the tip-sample interaction force. The use of a laser that is reflected on the back side of the cantilever and detected by the photodetector enables accurate determination of cantilever deflection. Two measurements are required to convert the signal of the photodetector into a quantitative value of force. *First*, the distance that the cantilever actually

deflects for a certain measured change in the photodetector voltage should be calculated. This value is slightly different each time the cantilever is put in the instrument due to the dependence on the optical path of the AFM detection laser, the laser intensity etc. *Second*, the cantilever spring constant needs to be obtained. This can be achieved by different methods; for example, through obtaining the resonance frequency of the cantilever (thermal calibration method). When the deflection, x, and spring constant, k, are known, the force can be calculated using Hooke's law:

$$F=kx$$

Different forces can be measured by AFM during a typical experiment, depending on the nature of the cantilever tip and the substrate. Some relevant forces using non-functionalized tips are presented in Table 2.1.

Table 2.1. Overview of interactions at different stages of the force spectroscopy. [modified from 16]

Approach	
Tip approaching (few μm)	- Electrostatic forces - Long-range interactions from absorbed molecules
Tip close to the surface (nm to atomic distances)	- Van der Waals - Chemical potential - Magnetic
Contact	
Tip indenting the sample	- Stiffness (Young's modulus, elastic response) - Viscoelastic response (variable rates or indentation depth)
Retract	
Tip lifting off surface (few atomic distances to nm)	- Non-specific adhesion (including chemical affinity, surface coatings)

The most commonly used model for measuring the elasticity of a sample is the Hertz model. The principles and assumptions of it are described in the next section. [15, 16]

2.2.1.1 Hertz Model

Hertzian Theory of Elastic Deformation was first described in 1881 by Heinrich Hertz. It relates the contact area between two curved bodies, which are brought into contact, to the elastic deformation properties of the materials. The Hertz model makes several assumptions. First of them is that the sample is isotropic; second that the body is treated as an elastic half space ("*an elastic half space is the term given to a flat surface on an infinite elastic solid",* [14]). Moreover, it is assumed that the indenter is not deformable and that there are no additional interactions between the indenter and the sam-

ple. Finally, the Hertz model assumes that the indentation is negligible comparing to the thickness of the sample so that the substrate does not influence the calculations. If the above mentioned conditions are met, the Young's modulus (E) of the sample can be calculated using the Hertzian model. The equation used is determined by the geometry of the indenter, which can be: parabolic, spherical, conical or four-sided pyramid (Figure 2.4). [13, 14, 15]

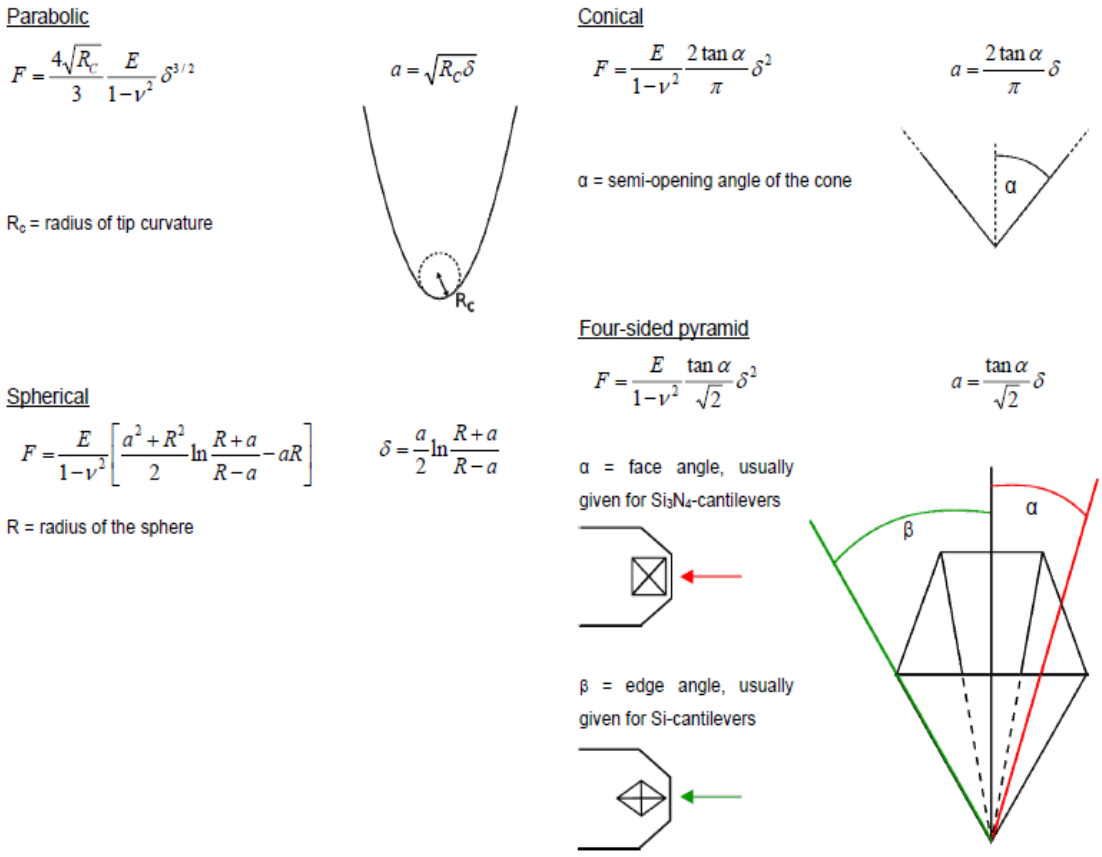

Figure 2.4. Different geometries of the indenters and their equations. [15]

The Young's modulus (E) is calculated by fitting the force indentation curves (F-δ curves) using E as a fit parameter. The contact point and the baseline can be either used as variable parameters or as fixed values when predetermined before. [15]

2.2.2. Oscillatory Rheology

Elasticity determination using AFM assumes that the material is purely elastic; however, in reality hydrogels are typically viscoelastic, with both a viscous and an elastic response. Oscillatory rheology is an important tool for studying and characterizing the mechanical behavior of viscoelastic materials due to its ability to quantify both the viscous and elastic properties. [17]

Oscillatory rheology is based on the induction of a sinusoidal shear deformation in the sample and the recording of the stress response. The sample is placed in between two surfaces (that can be have various geometries), one of which is stationary and another which is rotated by a motor imposing the time dependent strain $\gamma(t)=\gamma\sin(\omega t)$ on the sample. The time dependent stress $\sigma(t)$ is quantified by measuring the torque that the sample imposes on the moving surface. [17]

The difference between the elastic, viscous and viscoelastic materials can be observed when measuring the time dependent stress at a single frequency (Figure 2.5). For an ideal elastic solid the stress is proportional to the strain deformation, and the proportionality constant is the shear modulus of the material. The stress is exactly in phase with the applied sinusoidal strain deformation. In contrast, for the purely viscous fluid the stress in the sample is proportional to the rate of strain deformation, where the proportionality constant is the viscosity of the fluid. The applied strain and the measured stress are out of phase, with a phase angle $\delta=\pi/2$. [17]

Viscoelastic materials show a response that includes both in-phase and out-of-phase contributions. Consequently, the total stress response has a phase shift δ with respect to the applied strain deformation that lies between that of solids and liquids, $0<\delta<\pi/2$. [17]

The viscoelastic behavior of the system at the frequency of oscillation, ω, is characterized by the storage (elastic) modulus, $G'(\omega)$, and the loss (viscous) modulus, $G''(\omega)$, which respectively characterize the solid-like and fluid-like contributions to the measured stress response. For a sinusoidal strain deformation $\gamma(t)=\gamma 0\sin(\omega t)$, the stress response of a viscoelastic material is given by $\sigma(t)=G'(\omega)\gamma\, 0\sin(\omega t)+G''(\omega)\gamma 0\cos(\omega t)$. In a typical rheological experiment, the $G'(\omega)$ and $G''(\omega)$ are calculated as a function of omega, because whether a soft material is solid-like or liquid-like depends on the time scale at which it is deformed. [17]

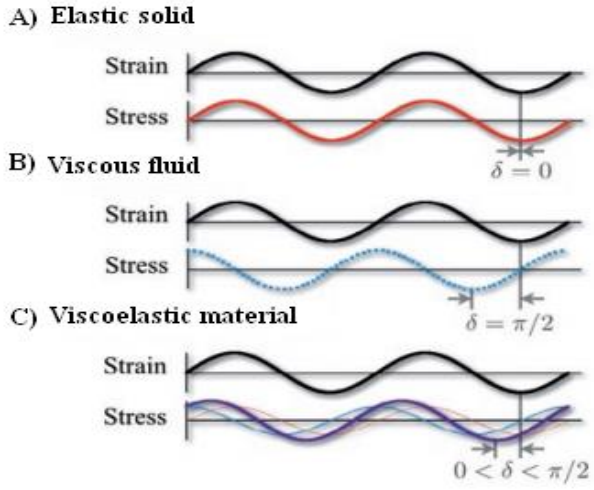

Figure 2.5. Schematic stress response to oscillatory strain deformation for: A) an elastic solid; B) a viscous fluid; C) a viscoelastic material. [modified from 17]

In particular, for hydrogel characterization, oscillatory rheology is a very convenient method that allows determination of the bulk mechanical properties of the material. The most common theory to relate bulk properties with the microscopic structure of a material is the Rubber Elasticity Theory, which states that the rubbery modulus scales roughly with the crosslinking density and temperature ($E \sim \rho T$). [18]

To utilize the rubber elasticity theory with oscillatory rheology, sinusoidal linear deformation measurements are made at low frequency rubbery regime to capture the shear modulus of the network. Thus, to be able to directly interpret the rubber elasticity theory the rheological measurements of elastic shear modulus G' must be nearly independent of frequency and of applied strain (i.e., in the linear viscoelastic regime). [18]

It is important to note that the relationship between Young's modulus, E, and shear (storage) modulus, G, is $E=2G(1+v)$. Furthermore, when a material can be assumed to be incompressible, its Poisson's ratio, v, approaches 0.5 and this relationship approaches $E \approx 3G$. [20, 21]

2.2.3. Swelling studies and mesh size calculations

An important property of hydrogels is their equilibrium swelling, which is linked to their mechanical characteristics. The swelling of the hydrogel is an increase in volume that occurs due to the hydrogel's ability to accommodate large amounts of water in its structure. Swelling largely affects the mechanical properties and the final hydrogel network architecture. Equilibrium swelling can be used to calculate the mesh size of the hydrogel. Mesh size can largely affect the diffusion of the molecules within the network, the proliferation and migration of encapsulated cells. [12]

In previous studies a correlation between the mesh size of a swollen cross-linked network and its volume in the swollen state was established and a theoretical model was designed. [12,19]

According to this model, the mesh size, ε, can be calculated based on the formula:

$$\varepsilon = V2,s^{-1/3}(\overline{ro}^2)^{1/2},$$

where *V2,s* is the polymer volume fraction of the gel in the swollen state and can be calculated:

$$V2,s = Vp/Vs$$

Unperturbed mean-square end-to-end distance of the PEG $(\overline{ro}^2)^{1/2}$ can be calculated as:

$$(\overline{ro}^2)^{1/2} = l(\frac{2\overline{Mc}}{Mr})^{1/2}Cn^{1/2}$$

In this formula *l* is the average bond length between C-C and C-O bonds in the repeat unit of PEG, taken as 1.46Å. $\overline{Mc}$ is the average molecular mass between the cross-links in the network, which is calculated based on the assumption that all the reactive groups of PEG react equally, and that the distribution of the other components between the PEG's arms is uniform. Therefore for the 1:0 4arm-PEG:2arm-PEG ratio the $\overline{Mc}$ was calculated as 10154 g/mol while for 1:8 ration it was calculated as 24770 g/mol. The schematic of calculation is shown in Figure 2.6. The molecular mass of the PEG unit *Mr* was the taken 44g/mol, and the characteristic ratio for PEG *Cn* was taken as 4 based on the literature [12, 19].

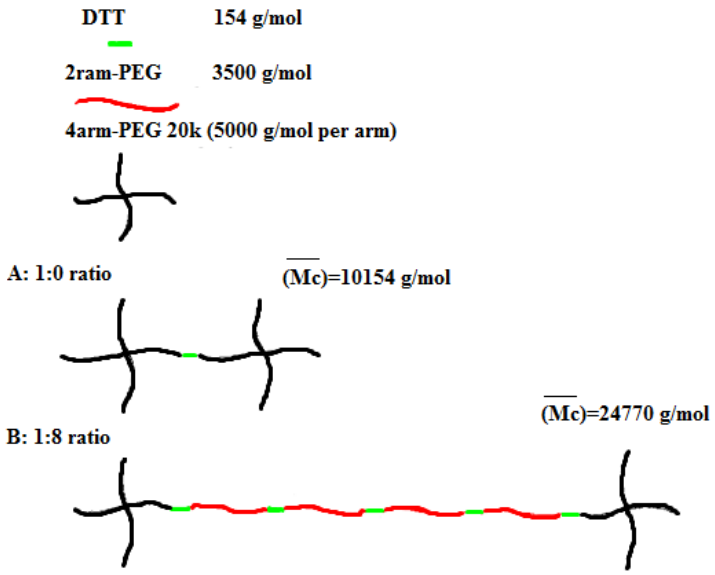

Figure 2.6. *Schematic of the calculation of the average molecular mass between the cross-links in the network. [own illustration]*

2.3. Cell lines

Cell lines derived from tumors and tissues are the most frequently used living systems in cell biology research. Due to limitations in the abundance of tissue samples, cell lines are often used in the studies of tumor-related phenomena. Cancer cell lines have been widely used in screening studies involving drug sensitivity and effectiveness of anticancer drugs. Other studies using cultured cells aimed at the determination of the phenotypic properties of cancer cells such as proliferation rates, migration capacity and ability to induce angiogenesis. [22]

2.3.1. LS174T cell line

The LS174T colon cancer cell line (Figure 2.7) is a trypsinised variant of the LS180 cell line; both lines were derived from a single patient: a 58-year old Caucasian female with Dukes type B adenocarcinoma of the colon. The cells have epithelial morphology, have microvilli and intracytoplasmic vacuoles. The cells are tumorigenic in nude mice. [23]

In vivo, tumors are often described as being ellipsoidal in shape [24, 25]. In vitro, this ellipsoidal tumor growth can be simulated with multiple cell lines. LS174T cells on the glass surface of the culture flask tend to grow in aggregates. When these cells are incorporated into a tissue-mechanics-mimicking hydrogel they tend to form agglomerates of spheroidal or ellipsoidal shape. It was hypothesized that the mechanical environment strongly influences the tumor shape development. [24, 25]

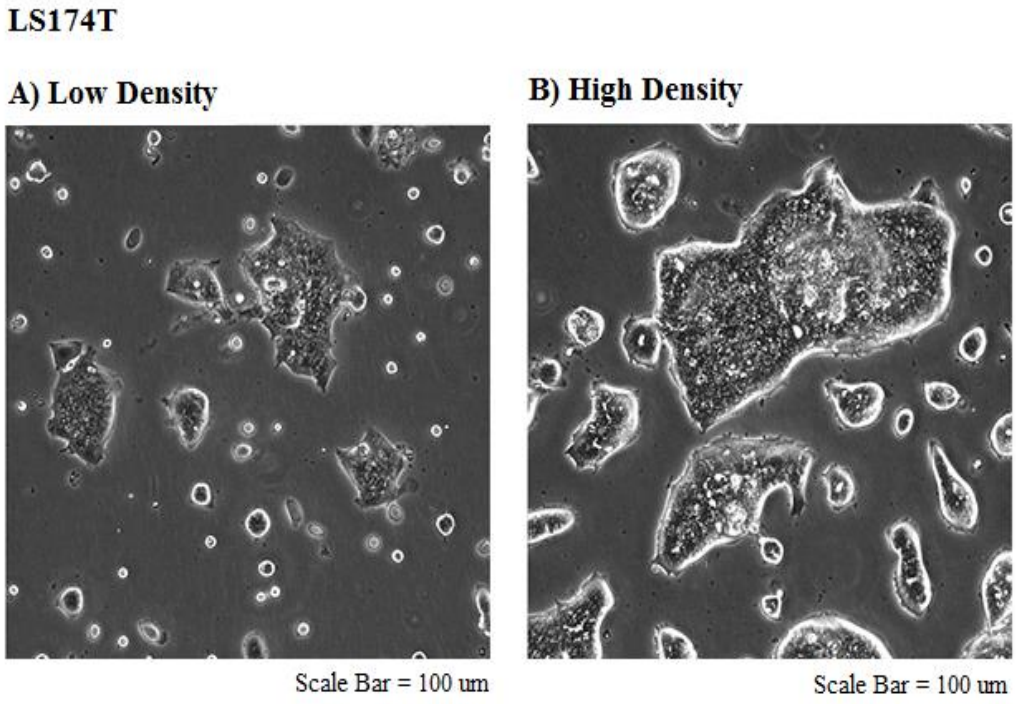

Figure 2.7. LS174T cell line in a culture at: A) low density, B) high density. [modified from 26]

3. Materials and methods

3.1. Materials

3.1.1. Materials for hydrogel formation

The following materials were used to prepare the different hydrogels for this project.

- **Poly(ethylene glycol)**

All poly(ethylene glycol) (PEG) precursors were purchased from JenKem Technology (Plano, USA)except from the 4arm-PEG-vs, which was obtained from Dimitris Missirlis. End-functionalization was confirmed by ^{1}H-NMR spectroscopy using Bruker Avance III 600 NMR-Spectrometer (Billerica, USA).

Two 4arm-PEG derivatives with two different end-functional groups were used as precursors: 4arm-PEG Vinyl sulfone (MW 20000 g/mol) (PEG vs 20k) and 4arm-PEG Maleimide (MW 20000 g/mol). In addition, two homobifunctional PEG derivatives end-functionalized with vinyl sulfones (MW 3500 g/mol) or maleimides (MW 3500 g/mol) were used. The chemical structure of these precursors is shown in Figure 1.1.

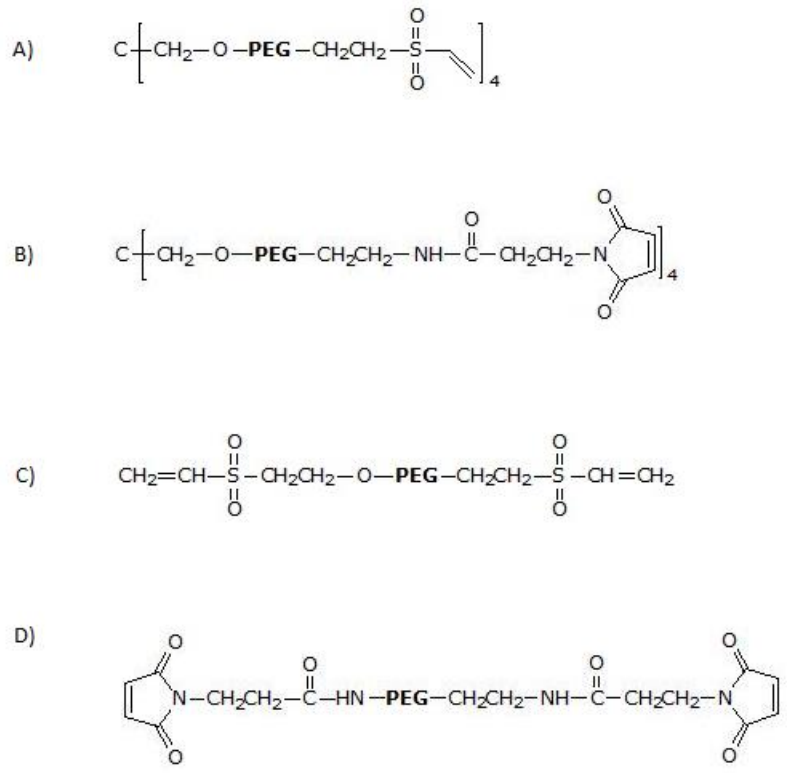

Figure 3.1. Chemical structure of PEG precursors. A: 4arm-PEG vinyl sulfone; B: 4arm-PEG maleimide; C: 2arm-PEG vinyl sulfone. D: 2arm-PEG maleimide [27]

● **DL-Dithiothreitol (DTT)**

DTT was purchased from Sigma-Aldrich (St. Louis, USA, Product No. D9779). The chemical structure of DDT (MW 154.25 g/mol) is shown in the Figure 1.2. The reactive groups of DTT are thiols.

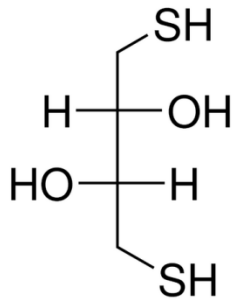

Figure 3.2. Chemical structure of DTT. [28]

● **Cleavable Matrix Metalloproteinase peptide (cMMP peptide)**

A peptide with a MMP cleavable site and two flanking cysteine residues was purchased from PSL GmbH (Heidelberg, Germany). Its amino acid composition was: GCRDGPQG↓IWGQDRCG (↓ is showing the cleavage site) [32]. The N-terminal group was acetylated and the C-terminal group was amidated. The molecular mass of the peptide was 1745.8 g/mol and its elemental composition C70H109N26O23S2.

● **Dulbecco's Phosphate Buffered Saline (PBS)**

PBS without calcium chloride and magnesium chloride was purchased from Sigma-Aldrich (St. Louis, USA, Product No. D8537). PBS is a buffer solution with physiological salt concentration, which is widely used in cell and tissue culture to maintain the pH within the physiological range: 7.2-7.6.

3.1.2. Materials for cell culture

The following cell culture media were used depending on the cell type used:

● **Eagle's Minimum Essential Medium**

Eagle's Minimum Essential Medium (EMEM) was purchased from ATCC (Wesel, Germany, Product No 30-2003) or Sigma-Aldrich (St. Louis, USA, Product No M2279) and contained, non-essential amino acids, 2 mM L-glutamine, 1 mM sodium pyruvate, and 1500 mg/L sodium bicarbonate. EMEM was supplemented with 10% Fetal Bovine Serum (FBS) and 1% Penicillin/streptomycin (Pen/strep). Media were sterile filtered prior to use.

● **Trypsin**

Trypsin-EDTA (0.05%) was purchased by Life Technologies (Carlsbad, USA, Product No 25300-054).

● **Accutase**

Accutase was purchased by Sigma-Aldrich (St. Louis, USA, Product No A6964).

● **L-Glutamine**

L-Glutamine (200 mM) was purchased by Life Technologies (Carlsbad, USA, Product No 25030-024)

● **Fetal Bovine Serum**

Fetal Bovine Serum (FBS) was purchased by Sigma-Aldrich (St. Louis, USA, Product No F7524)

● **Penicillin Streptomycin**

Penicillin Streptomycin (Pen/Strep) was purchased by Life Technologies (Carlsbad, USA, Product No P4333). It contains 10000 units/ml of penicillin and 10000 µg/ml of streptomycin.

3.1.3. Other materials

● **Ellman’s Reagent (5,5'-dithio-bis-(2-nitrobenzoic acid))**

Ellman’s Reagent (≥98%) was purchased by Sigma-Aldrich (St. Louis, USA, Product No D8130). The molecular mass of it was 396.35 g/mol.

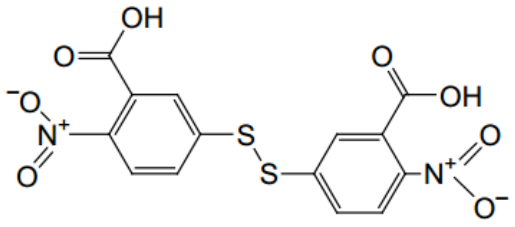

Ellman's Reagent;
5,5'-Dithio-*bis*-(2-nitrobenzoic acid)
$C_{14}H_8N_2O_8S2$
Mol. Wt.: 396.35

Figure 3.3. Structure of Ellman's reagent. [29]

- **Cysteamine**

Cysteamine (approximately 95%) was purchased by Sigma-Aldrich (St. Louis, USA, Product No M9768). The chemical structure of cysteamine (MW 77.15 g/mol) is shown in Figure 3.4.

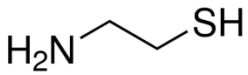

Figure 3.4. The chemical structure of cysteamine. [33]

- **Ethylenediaminetetraacetic acid tetrasodium salt dehydrate**

Ethylenediaminetetraacetic acid tetrasodium salt dehydrate (EDTA) (99.0-102.0%) was purchased by Sigma-Aldrich (St. Louis, USA, Product No ED4SS). The chemical structure of EDTA (MW 416.20 g/mol) is shown in Figure 3.5.

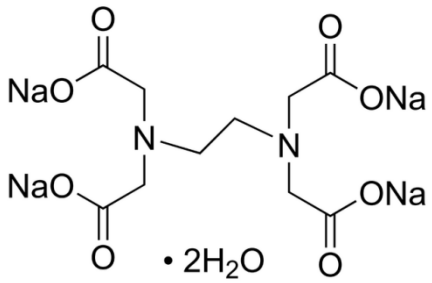

Figure 3.5. The chemical structure of EDTA. [35]

- **Reaction Buffer for Ellman's Reagent experiment**

Reaction Buffer is prepared with 0.1M sodium phosphate, pH 8.0, containing 1mM EDTA.

● **(3-Aminopropyl)triethoxysilane)**

(3-Aminopropyl)triethoxysilane (APTES) (≥98%) was purchased by Sigma-Aldrich (St. Louis, USA, Product No A3648). Its molecular weight was 221.37 g/mol. In the Figure 3.6 the chemistry performed by APTES-coating is shown.

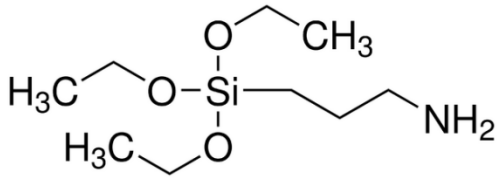

Figure 3.6. The structural formula of (3-Aminopropyl)triethoxysilane (APTES). [34]

● **FluoSpheres carboxilate-modified**

FluoSpheres (2% solids, 2mM azide) were purchased by Life Technologies (Carlsbad, USA). Two different types of beads were used: 100 nm blue (Product No F8797: actual size 100 nm, 350/440 nm) and 20 nm dark red (Product No F8783: actual size 28 nm, 660/680 nm).

● **Dextran Oregon green 488**

Dextran (MW 70000 g/mol, 496/524) was purchased by Life Technologies (Carlsbad, USA, Product No D-7173). It was dissolved at concentration 5mg/ml in PBS.

● **Live/dead viability kit**

The live/dead viability kit was purchased by Life Technologies (Carlsbad, USA, Product No L-3224). It consists of two different dyes: Calcein AM and Ethidium homodimer-1. Calcein (494/517) is at the 4mM concentration, and Ethidium homodimer-1 (528/617) is at 2mM concentration.

3.2. Methods

3.2.1. Hydrogel Formation

Michael-type donors (thiol-containing precursors) and Michael-type acceptors (vinyl sulfones or maleimides-containing precursors) were dissolved in PBS. Precursor solutions were mixed to give a final donor:acceptor molar ratio of 1:1. Precursor concentration was varied by mixing with PBS, when required. A typical precursor volume for hydrogel formation was 40 µl.

Freeze dried aliquots of PEG vs precursors were prepared and stored at -20°C prior to use in order to ensure reproducibility. A large amount of PEG precursor was weighed, dissolved in milliQ water (solution with concentration of 2 wt% PEG was prepared) and the resulting solution sonicated and frozen (-80 °C). Samples were freeze-dryed using FreeZone Plus 2.5 Liter Cascade Benchtop Freeze Dry System from LABCONCO. An attempt to aliquot DTT in the same manner failed and therefore it was dissolved each time prior to gel formation. The cMMP peptide was successfully aliquoted by dissolving the peptide at concentration 1 mg/ml. The pH of the aliquoted solution was adjusted to be approximately 7, by adding small amounts of sodium hydroxide and/or hydrogen chloride. Depending on the experiment type, gels were formed either on APTES-coated glass dishes (see section 3.2.2) or in Eppendorf tubes.

3.2.2. Surface silanization

Coating of glass substrates by APTES was performed by vapor deposition. Dry glass surfaces were placed into a dessicator with a small glass dish containing APTES (2-3 ml). The dessicator was sealed, placed under mild vacuum and left overnight. Dishes were removed and stored at room temperature until further use. A schematic of the silanization process is shown in Figure 3.7.

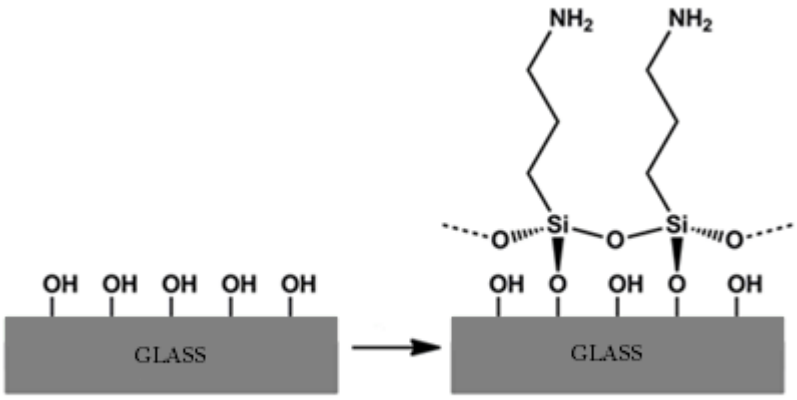

Figure 3.7. Schematic of silanization: surface modification by APTES-coating. [modified from 30]

3.2.3. Time to gelation

An important parameter that characterizes hydrogel formation is the gelation kinetics. In order to measure the time required for gelation, the following protocol was applied: gel precursors were mixed in Eppendorf tubes and periodically inspected visually for signs of gelation. Specifically, a pipette tip was gently inserted in the precursor mixture till

the very bottom of the Eppendorf tube and then slowly retracted. When material adhered to the tip, forming a line, we considered a gel had started to form. In this way, we initially measured for each formulation the time to gelation with a five minutes precision. Next, new samples were prepared and precision was enhanced by inspecting samples every minute (around the previously obtained gelation time). Typically four samples were measured in parallel, about three sets were measured for each of the hydrogel formulations.

3.2.4. Swelling Study

Swelling measurements were performed as following: gel formulations (40 µl) were prepared in preweighed Eppendorf tubes. The exact precursor mass was measured by weighing the Eppendorf tubes with the precursors and consequently subtracting the tube mass. Gelation was left to proceed at room temperature for two hours, after which 350µl of MilliQ water were carefully added in each tube and gels were left to swell at room temperature. After approximately 96 hours, the liquid above the gels was carefully removed from the Eppendorf tubes and these were weighed. The volume in the swollen state (*Vs*) was calculated assuming a density of 1 g/cm^3 (the density of water) and multiplying it with the obtained gel mass in the swollen state. The dry volume *(Vp)* was calculated assuming a density of 1.12 g/cm^3 (the density of PEG 20k) and multiplying it with the dry polymer mass obtained from the measurement [31].

Based on the theoretical models designed in the previous studies (see section 2.2.3) the average mesh sizes for different formulations were calculated.

3.2.5. Atomic Force Microscopy (AFM)

AFM measurements were performed using the NanoWizard3 AFM (JPK Instruments), which was mounted on a Zeiss Axiovert200 inverted microscope.

The cantilever used was produced by SQube (type CP-FM-BSG-B-5). It was a FM-Silicon-SPM-Sensor with colloidal particle of a 10 µm diameter (range ±10%). The technical data of the cantilever is presented in the Table 3.1.

Table 3.1. Technical data of the AFM cantilever.

Material	Borosilicate glass
Thickness	3.0±1 µm
Length	225±10 µm
Width	28±7.5 µm
Resonance frequency	45-115 kHz
Force constant	0.5-9.5 N/m

Prior to the measurements, the sensitivity was obtained. It is showing how much the cantilever deflects when the certain force is applied and correlates the voltage on the

detector with the known displacement. We need to know the sensitivity in order to obtain the spring constant. Knowing the spring constant we can obtain the force which, in its turn, is needed to be able to calculate the Young's modulus.

First, we measured the sensitivity in air on the stiff non-deformable substrate (glass). Based on this value the spring constant was determined using the "thermal-noise method". The range of the spring constants measured for all of the experiments was 1.63-1.73 N/m. Next step was to measure the sensitivity in liquid (in our case in PBS) since it depends on the medium in which it is measured due to the different laser beam refraction. The spring constant is supposed to remain the same independently form the medium.

The measurement procedure for hydrogels is next described. First, the cantilever was brought into contact with the surface. Then, force-distance curves were obtained with an indentation depth of at least 500 nm. Finally, the force-distance curves were analyzed using the JPK-data processing software: the curves were smoothed, the baseline corrected and the contact point was automatically found. Then, the Young's modulus was determined using the Hertz model which is described in section (2.2.1.1). Typically, ten curves per position and at least three positions for one gel were measured; for each formulation at least two gels were prepared. For incompressible materials the Poisson ratio is known to be 0.5, therefore, we have chosen this value for our experiments. [21].

3.2.6. Oscillatory Rheology

Oscillatory rheology was performed on a Kinexus instrument (Malvern Instruments Ltd, Malvern, UK) in order to characterize the bulk mechanical properties of the materials. For the experiment the sample was placed between two parallel plates (the upper plate was 8 mm in diameter) in a humidified chamber (in order to prevent dehydration of the precursor solution). The gels were formed *in situ*, i.e. the gel precursors were directly pipetted on the bottom plate of the rheometer and then the upper plate was lowered so that the precursor mixture was squeezed between the two plates. For 40 µl precursor mixtures and the geometry used, the gap between the two plates, and therefore the thickness of the formed gel was 0.75 mm.

Three types of measurement were performed. First, a measurement was performed at constant frequency and shear strain to obtain the shear elastic G' and viscous G" modulus and to determine the liquid-to-solid transition point (G'-G" crossover). [18] This initial measurement lasted 60 minutes. Next, a frequency sweep at constant strain (from 20 Hz to 0.02 Hz, 1%) measurement was performed, and finally a strain amplitude sweep at constant frequency (from 0.02% to 20%, 1 Hz).

3.2.7. Quantitating sulfhydryl groups with Ellman's reagent

Ellman's reagent experiments were performed in order to check the amount of free thiols on DTT or peptides as well as unreacted thiols in the hydrogels.

A calibration curve was constructed with cysteamine standards, prepared by dissolving cysteamine in water at different concentrations. A set of test tubes containing 1.25 ml of Reaction Buffer (see section 3.1.3) and 25 µl of Ellman's Reagent Solution (Ellman's reagent was dissolved in the Reaction Buffer at concentration 4 mg/ml [29]) was prepared. After that, 100 µl of each standard or unknown were added to one of the test tubes, the solutions were mixed and incubated at room temperature for 15 minutes. The absorbance at 412 nm wavelength was measured on the 96-well plate using TECAN infinite M200. For each of the standards or unknown 100 µl of the solution from above the gels were carefully transferred onto the 96-well plate, and the absorbance was measured at 412nm wavelength using TECAN infinite M200 (three measurements for each well). [29]

Furthermore, the Ellman's Reagent experiment was performed to estimate the percentage of free thiols in the formed gels. In this case, the Ellman's reagent reacted with free thiols that were present in the hydrogel after the cross-linking reaction. Gels of different concentrations were prepared (10% and 5%, n=3) and incubated at room temperature for 2 hours for the cross-linking reaction to proceed. Meanwhile the Ellman's stock solution was prepared by dissolving the Ellman's reagent in the Reaction Buffer at concentration 200 µg/ml. After 2 hours, 300 µl of the Ellman's stock solution were carefully added to the Eppendorfs with gels and were left overnight in the 4°C protected from light. A calibration curve was prepared using appropriate concentrations of Ellman's stock solution and cysteamine standards. 100 µl of the Ellman's stock solution from above the gels were carefully transferred onto the 96-well plate (two wells for each of the samples) and the absorbance at 412 nm wavelength was measured and averaged from three measurements per each well.

3.2.8. Beads encapsulation

The actual pore size of hydrogels can be qualitatively evaluated by encapsulating beads of different sizes into the gel and observing their mobility. For this purpose, fluorescent carboxylated nanobeads were sonicated, diluted to two different concentrations (1:1000 and 1:10000) and encapsulated (2 µl) into gels, prepared according to the standard procedure. The gels used were 5% gels prepared from the aliquots: 4arm-PEG vs 20k with 2arm-PEG vs 3.5k and DTT at 1:8 ratio. After mixing of the components 15 µl of the solution were carefully transferred onto the APTES-coated dish, protected from light by aluminum foil and left for the cross-linking reaction to proceed. After approximately 2 hours the mobility of the beads was checked using the Leica DM6000B inverted microscope with either 40x dipping objective or 63x oil objective. Further, the

gels were covered with PBS and left to swell for several days after which the mobility was checked again in the swollen state.

3.2.9. Dextran diffusion

The diffusion of macromolecules (dextran) outside the gels was performed to further evaluate the actual pore size of the network.
To evaluate the actual pore sizes the diffusion of macromolecules (dextran) outside from the hydrogels was studied.
Dextran was diluted to 5 mg/100 ml concentration and encapsulated (1 µl) into the gels (10 µl) which were prepared in Eppendorf tubes according to the standard procedure. The gels used were PEG 20k vs 5% and 10% gels at 1:0 4arm-PEG:2arm-PEG ratio prepared from aliquots. The formulations were left for the cross-linking reaction to proceed for 2 hours at room temperature, after which 1ml of water was added on top of each gel. At specific time points, 25 µl of liquid were taken from the "sink" (the solution above the gel), placed into small Eppendorf tubes and kept protected from light at 4°C. After all of the samples were collected, their fluorescence intensity was measured using a TECAN infinite M200 well plate reader (496 nm excitation wavelength and 524 nm emission wavelength).

3.2.10. Cells sub-culturing method

The LS174T colon cancer cell line was kindly provided by Dr. K. Mills (MPI Stuttgart). The cells were cultured at 5% CO2 and 37°C in EMEM supplemented medium (see section 3.1.2). Sub-confluent cell cultures were split at a ratio between 1:10 and 4:10 using trypsin-EDTA (0.05% trypsin) every second day or when the culture became confluent enough (70-80%).

3.2.11. Cell encapsulation

All the materials required for the encapsulation were prepared, sterilized with ethanol and put into the culture hood. The vinyl sulfones and thiols were dissolved in PBS and set aside.

Cells were washed once with PBS, detouched from the culture flask surface by applying 1 ml of accutase, and incubated for 5 minutes at 37°C. Cells were then suspended in 4ml of non-modified EMEM and centrifuged for 4 minutes at 1200 rounds per minute. Following centrifugation the supernatant was aspirated and cells were resuspended in non-modified EMEM. Cells were counted using a Hemacytometer. Cell suspensions with the desired amount of cells (typically 20000 cells/ml concentration) were prepared and kept on ice until addition to gels.

The vinyl sulfones were mixed with thiols and left for the cross-linking reaction to proceed for different time periods prior to cell addition. Cells (1-2 µl) were then gen-

tly added to the gel precursors, mixed by slowly pipetting, and a droplet was carefully pipetted on the APTES-coated glass dish. Gels with encapsulated cells were left in the incubator at 37°C for one hour before modified EMEM was added on top of the gel.

The gels were checked under the microscope several hours after the encapsulation in the controlled environment (5% CO_2 and 37°C). The checking was done by taking images every 20 seconds for 5-10 minutes time-loops and observing the cells activity.

3.2.12. Cell viability

Cell viability experiment was performed using the live/dead viability assay. LS174T cells were seeded onto the 96-well plate one day before the experiment, and left to attach and spread. Concentrations of precursors comparable to those in the gels (1000ug/ml for PEG and 500 µg/ml for DTT) were prepared in non-modified cell culture medium. Seeded cells were covered with the prepared solutions (two samples for each condition) and left in the incubator (37°C, 5% CO2) for 30 minutes. After the incubation cells were carefully washed with PBS (two times for 5 minutes each), the mix of dyes from the live/dead viability kit was applied on top of them, and cells were incubated for 30 minutes (protected from light). Calceine dye was diluted with PBS to be 4 µM and EthD was diluted to be 2 µM. Following the incubation cells were carefully washed three times and then checked under the microscope.

3.2.13. Imaging

Cell survival and growth were checked by performing phase contrast imaging using a Delta Vision system (Applied Precision Inc.) on an Olympus IX inverted microscope equipped with a cooled CCD camera. The images were obtained with 10x and 20x air objectives. Live cell imaging was performed at 37 °C and 5% CO_2.

Encapsulated beads were observed using Leica DM6000B upright microscope equipped with a CCD camera. Oil immersion 63x/1.4 NA and water immersion 40x/0.8 NA dipping objectives were used.

Microscopy images were analyzed using the public domain Java-based software ImageJ.

4. Results

4.1. Reagent characterization

In this project, a Michael-type addition reaction of unsaturated double bonds to thiols was used to prepare hydrogels. Bi-functional, thiolated small molecules or peptides served as Michael-type donors, while multi-arm precursors functionalized with vinyl sulfones or maleimides served as the Michael-type acceptors. Donors were mixed with acceptors at different molar ratios to prepare hydrogels of different composition and concentration. The reaction occurred in a phosphate buffer (PBS) to maintain pH in the physiological range (7.2-7.6) and at room temperature unless otherwise noted.

Initially, the amount of free thiols on DTT or peptides used in the reaction was quantified using the Ellman's reagent test. Sample concentration was calculated based on a calibration curve using cysteamine standards (Graph 4.1).

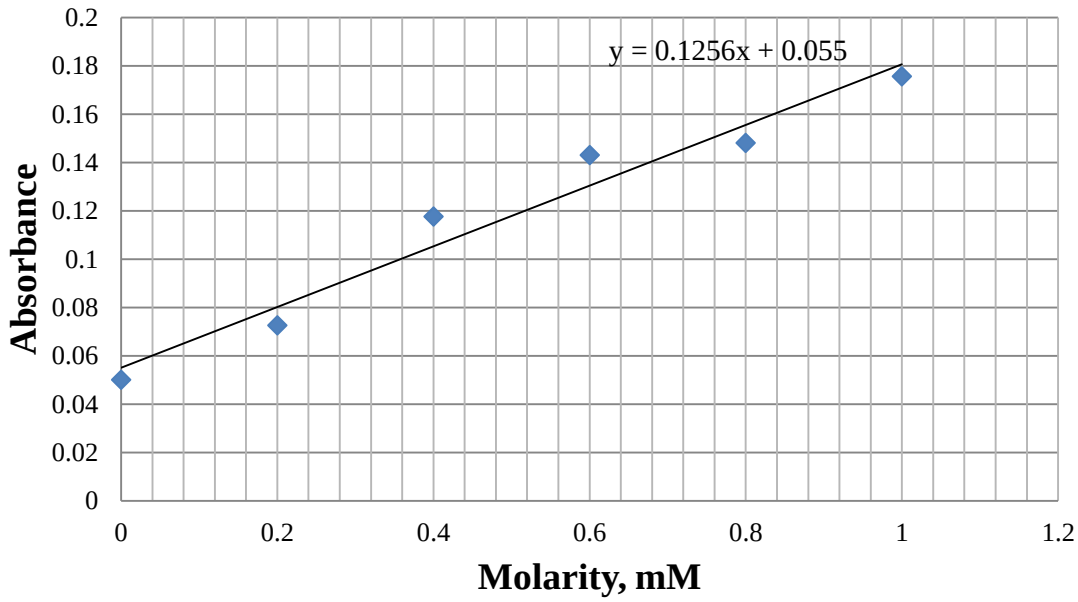

Graph 4.1. Standard curve for Ellman's Reagent test.

Furthermore, the Ellman's reagent measurement was performed for the peptide (Graph 4.2) or DTT (Graph 4.3) at different time points (0, 5, 10, 15, 20 and 30 minutes). Our results showed that the amount of free thiols in the dissolved peptide (Graph 4.2) or DTT (Graph 4.2) did not change significantly over time. Therefore, we conclude that the thiol concentration is stable and no significant amount of disulfides has formed in this time period.

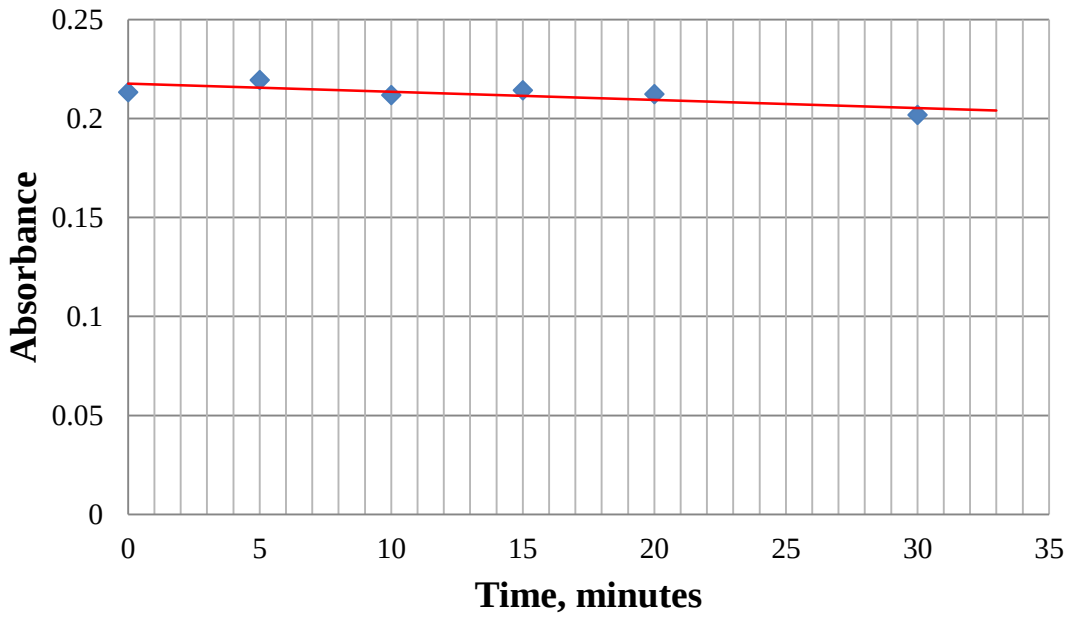

Graph 4.2. Changing of the absorbance of Ellman's reagent that has reacted with peptide over 30 minutes time interval.

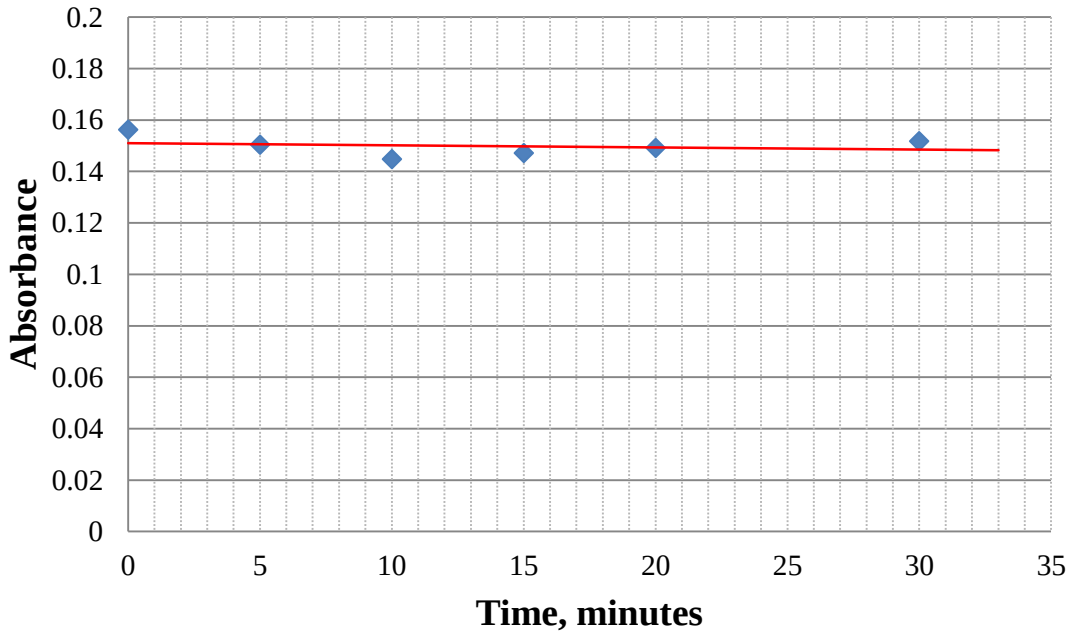

Graph 4.3. Changing of the absorbance of Ellman's reagent that has reacted with DTT over 30 minutes time interval.

Moreover, Ellman's reagent measurement was performed for quantifying the amount of unreacted thiols in the gels. A calibration curve using cysteamine standards was obtained (Graph 4.4).

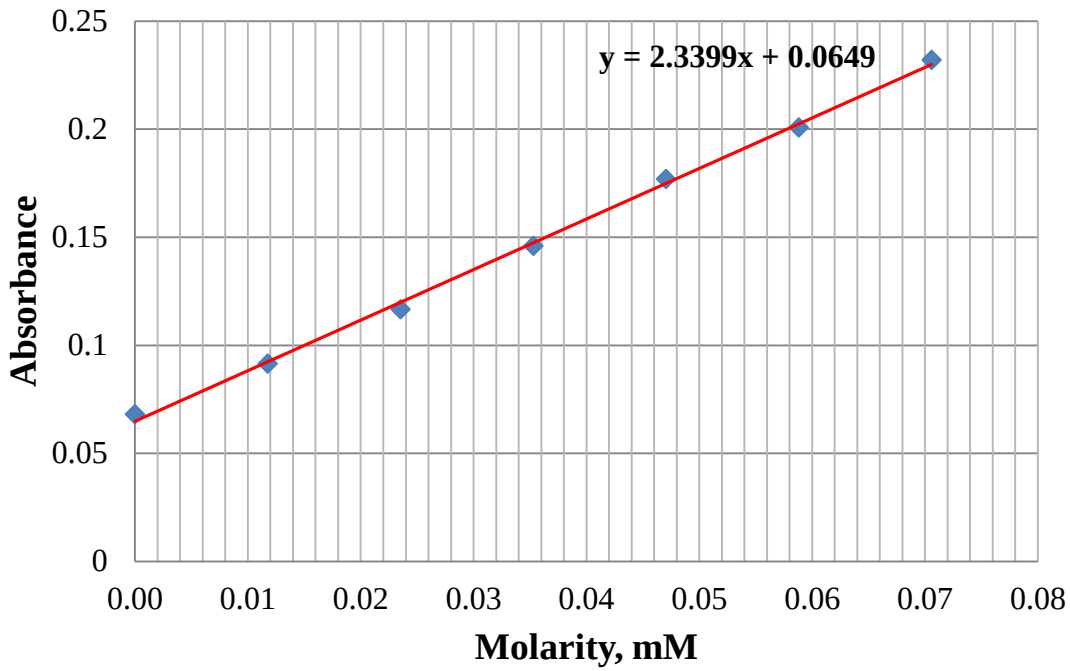

Graph 4.4. Standard curve for determination of free thiols in the gels with Ellman's Reagent.

The molarity of free thiols was calculated based on the equation of the trend line of the calibration curve. The percentage of free thiols in the gels was calculated based on this molarity (Table 4.1).

Table 4.1. Percentage of free thiols in the gels.

Gel formulation	Percentage of free thiols
5%	3.91
10%	2.51

4.2. Gel Formation

An important goal of this project was to control the pore size of gels, with a focus on obtaining large pore sizes. Initially, we decided to vary the weight concentration of the precursor solution and examine how this parameter affects gel formation and structure. In all formulations, the value of "%" refers to the weight concentration of 4-arm PEG (VS or maleimide) in the precursor, which was reacted with a 1:1 molar ratio with thiol-containing molecules. We expected that with lower concentration, swollen gels would be softer, with higher pore sizes. However, below a certain concentration, gelation will not be possible because the network would not be able to form. As shown in Table 4.2, gelation of PEG 20k vs and PEG 10k vs with DTT depended on both concentration and molecular weight of the 4-arm PEG vs. Gelation for PEG 10k vs oc-

curred at concentrations equal or above 5% while for PEG 20k vs a concentration of at least 7.5% was required for gel formation. At the same time, gelation was significantly faster for 10k vs formulations compared to the 20k vs ones, at the same concentration (Table 4.2).

Table 4.2. Gelation ranges for PEG 20k vs and PEG 10k vs with DTT.

Formulation	Gelation within 90 minutes	Time to gelation, minutes
4arm-PEG vs 20k+DTT		
15%	yes	50-60
10%	yes	60
7.5%	yes	60-90
5%	no	
4arm-PEG vs 10k+DTT		
15%	yes	15
10%	yes	20
7.5%	yes	30
5%	yes	60
3%	no	

This initial attempt to identify the gelation range and kinetics revealed some reproducibility issues. In order to minimize weighing errors, dilution effects and ensure reproducibility, we decided to prepare lyophilized aliquots of PEG precursors. Additionally, we focused only on the larger PEG (20k vs), which was expected to produce softer gels. Using aliquoted PEG 20k vs, gels were formed even at the concentration of 5%, in a reproducible fashion (Table 4.3). Moreover, gelation times were significantly shorter compared to the nonaliquoted samples (Table 4.3).

Table 4.3. Gelation of the aliquoted PEG 20k vs with DTT.

Formulation	Gelation within 90 minutes	Time to gelation (range), minutes
4arm-PEGvs20k(aliquoted)+DTT		
10%	yes	18 (13-20)
5%	yes	50 (45-54)
3%	no	

Next, we incorporated a linear (2arm)-PEG 3.5k vs into the hydrogel network in an attempt to increase pore size and examined gel formation. At first, a molar ratio of 1:2 (4arm-PEG:2arm-PEG) was selected. However, the differences from the control sample were not very pronounced. Therefore, we next used a molar ratio of 1:8. Gela-

tion times for the 1:0 ratio and 1:8 ratio were comparable. In case of 5% 1:8 ratio gels there was a reproducibility issue regarding gel formation: the gels were occasionally not forming at all. This means that the gel formation threshold lays close to 5% for these gels.

Table 4.4. Gelation of the aliquoted PEG 20k vs and incorporated linear PEG 3.5k vs at 1:8 ratio with DTT.

Formulation	Gelation within 90 minutes	Time to gelation, minutes
4arm-PEG vs 20k(aliquoted)+2arm-PEG vs 3.5k(aliquoted)+DTT 1:8 ratio		
10%	yes	18-19
5%	occasional	49-53

Besides the effect of concentration and linear PEG incorporation on gel formation, we examined how different PEG functionality would affect the process of gelation. The chemistry was changed via replacing the vinyl sulfones on PEG with maleimides. An attempt to aliquot PEG maleimide was made; however, addition of PBS to the freeze dried, aliquoted PEG led to gelation, presumably due to PEG maleimide polymerization. Therefore, PEG maleimide was weighed before each experiment.

The time to gelation was checked for PEG maleimide gels the same way as previously in order to identify the gelation range and gelation threshold (Table 4.5). Gelation with PEG maleimide precursors occurred at concentrations equal or above 2%, significantly lower than the concentration required for PEG vs-based gels. Moreover, the reaction proceeds very rapidly (almost instantaneously, meaning that gels form immediately after the addition of precursors together), which is very different from the PEG vs behavior, where even at higher concentrations (10%) gel formation takes about 20 minutes.

Table 4.5. Gelation of the PEG maleimide with DTT.

Formulation	Gelation within 90 minutes	Time to gelation, minutes
4arm-PEG maleimide 20k+DTT		
15%	yes	instantaneous
10%	yes	instantaneous
7.5%	yes	instantaneous
5%	yes	instantaneous
4%	yes	instantaneous
3%	yes	instantaneous
2%	yes	instantaneous
1%	no	

Next, we incorporated a linear (2arm)-PEG 3.5k maleimide into the hydrogel network alike with the PEG vs experiments. In this case, incorporation of linear PEG chains shifted the gelation threshold concentration above 3% (Table 4.6). Moreover, gelation times increased to several minutes comparing to the instantaneous gelation of the 1:0 ratio formulations. Nevertheless, gelation times of PEG maleimides at 1:8 ratio are significantly shorter than those of PEG vs at the same ratio and concentrations.

Table 4.6. Gelation of the PEG maleimide at 1:8 ratio with DTT.

Formulation	Gelation within 90 minutes	Time to gelation, minutes
4arm-PEG maleimide 20k+2arm PEG maleimide 3.5k+DTT 1:8 ratio		
10%	yes	3-4
5%	yes	5-10
3%	no	

Furthermore, we decided to try a new approach in order to try to slow down the gelation and to get more reproducible results. We were first reacting the linear PEG maleimide with DTT, and then cross-linking the resulted chains with the 4-arm PEG. Linear PEG was mixed with DTT and kept for two different periods of time before 4arm-PEG addition, in order to determine how the reaction time affects hydrogel formation. This method affected the gelation range: 3% gels were forming at a 1:8 ratio (Table 4.7), unlike those where all precursors were mixed at the same time (Table 4.6). Moreover, the time to gelation decreased. The duration of reaction between the bifunctional PEG and DTT seemed to slightly affect the time to gelation: gelation was faster

for gels when the two precursors were mixed for 15 minutes prior to 4-arm PEG addition compared to when they were mixed for 5 minutes.

Table 4.7. Gelation of the PEG maleimide with the preproduced the long 2PEG-DTT chains.

Formulation	Gelation within 90 minutes	Time to gelation, minutes
(Linear PEG 3.5k maleimide+DTT)+4arm-PEG maleimide		
5% (15minutes to react)	yes	instanteneous
5% (5 minutes to react)	yes	instanteneous
3% (15minutes to react)	yes	20
3% (5 minutes to react)	yes	35

4.3. Gel formation measured by oscillatory rheology

Oscillatory rheology was used to determine the liquid-to-solid transition and measure gelation kinetics of selected formulations in a more precise manner. The liquid-to-solid transition measured by the oscillatory rheology is presented in Table 4.8.

Table 4.8. Time to gelation via rheology measurements.

Formulation	Time to gelation, minutes
PEG 20k vs + DTT	
10%	7
PEG 20k vs + DTT	
5%	26

The time required for gelation determined by the rheology measurements was significantly shorter compared to the one recorded by visual observation (Table 4.3). This is most likely due to the fact that during the rheology measurement we are constantly adding energy to the system through mixing/shearing of the reactants in the rheometer.

Graphs 4.5 and 4.6 show the evolution of storage and loss moduli with time for the 10% and 5% gels, respectively. When the shear elastic (storage) modulus reaches the plateau in the graph this indicates that the network formation is completed. However, in our case the plateau was not reached during the 60-minute observation time. Nonetheless, they allow observing the gelation kinetics and differentiating between the gels. It can be

seen that for 10% gel (Graph 4.4) the storage modulus curve is much steeper and plateau is almost reached within one hour while for 5% gel (Graph 4.5) the storage modulus curve is still increasing. It can be seen that the relative increase of the storage modulus decreases with time.

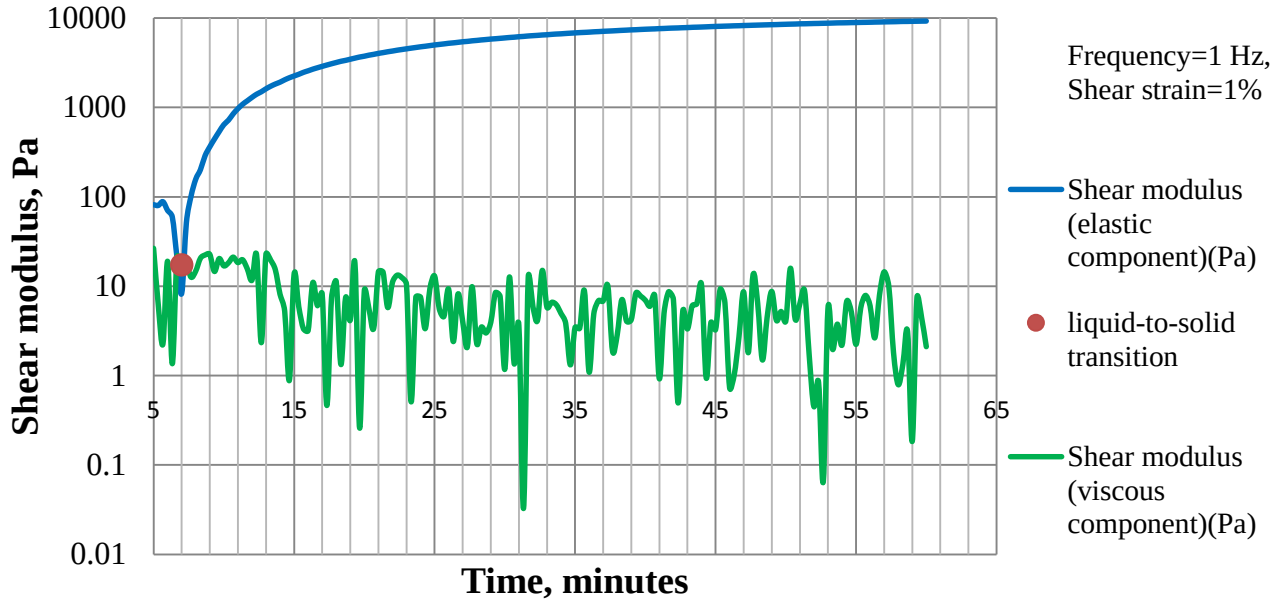

Graph 4.5. The gelation kinetics of the 10% gel measured by oscillatory rheology: shear modulus (elastic and viscous components) and point of liquid-to-solid transition.

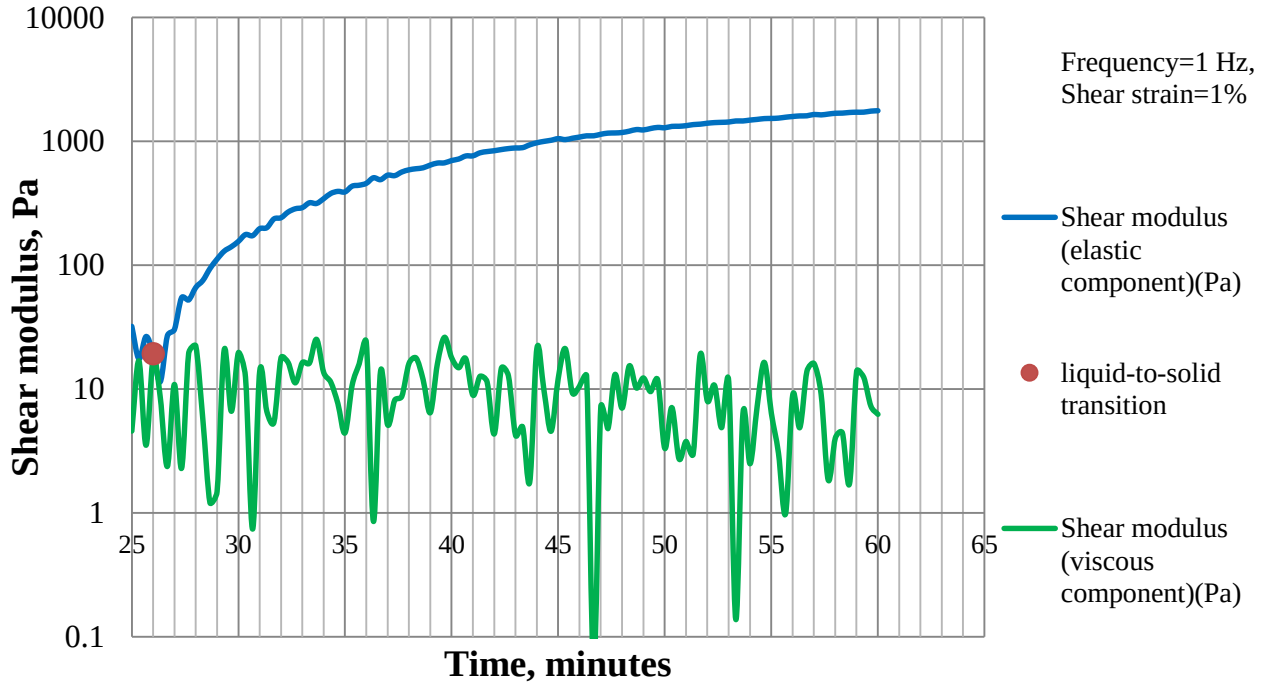

Graph 4.6. The gelation kinetics of the 10% gel measured by oscillatory rheology: shear modulus (elastic and viscous components) and point of liquid-to-solid transition.

4.4. Young's modulus measured by oscillatory rheology

The strain amplitude sweep measurements (Graph 4.7. and Graph 4.8.) were performed after the gelation kinetics experiments (in the non-swollen state) in order to ensure that elastic shear modulus G' is nearly independent of frequency (i.e., in the linear viscoelastic regime). Our results show that the storage modulus is independent from the applied strain.

We extracted the elastic modulus values from these experiments and calculated the Young's modulus from them. Even though we are not sure the gelation is complete at this time point, these values allowed us to compare the different conditions as well as the two different characterization techniques (AFM & Rheology). As was mentioned before (section 2.2.2), the relationship between the elastic shear modulus, G', and Young's modulus, E, is E=2G'(1+v). We assumed a Possion ratio of 0.5 (incompressible material, see section 2.2.2) and therefore E ≈ 3G'. [20, 21] G' values obtained in strain amplitude sweep experiment can be related to the Young's modulus (Table 4.9).

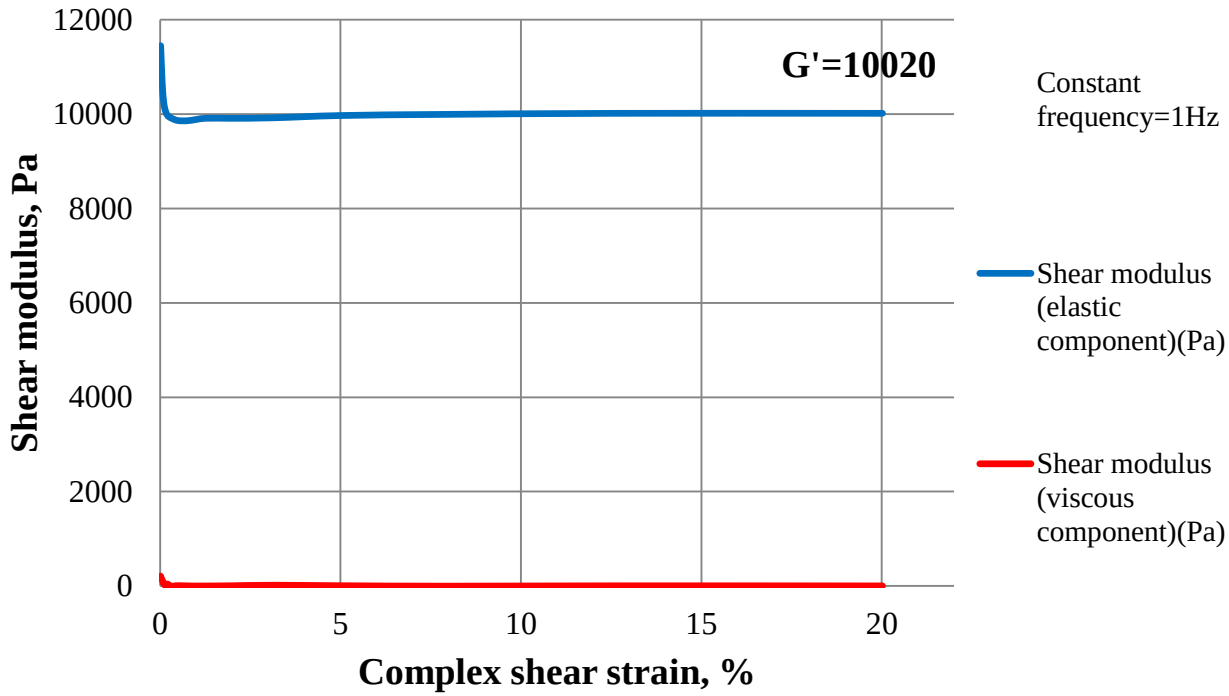

Graph 4.7. Strain amplitude sweep graph for 10% PEG vs hydrogel at 1:0 4arm-PEG vs:2arm-PEG vs ratio.

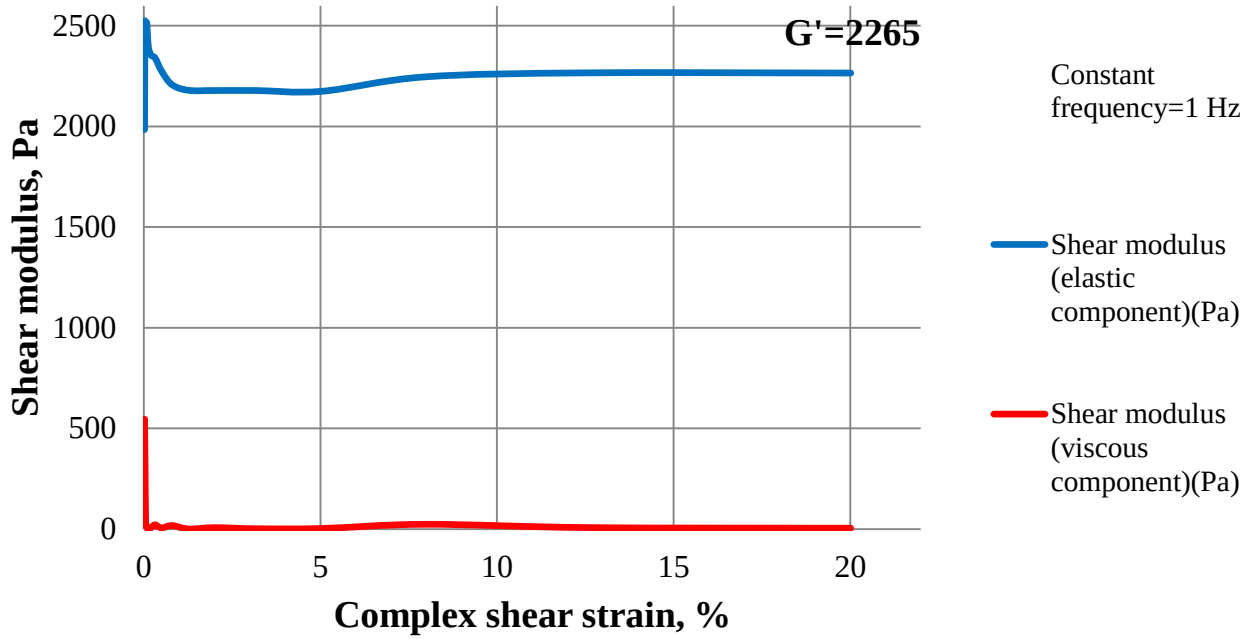

Graph 4.8. Strain amplitude sweep graph for 5% PEG vs hydrogel at 1:0 4arm-PEG vs:2arm-PEG vs ratio.

Table 4.9. Relation of the elastic modulus values obtained by oscillatory rheology to the Young's modulus.

Elastic shear modulus	Young's modulus
5% PEG vs gel at 1:0 ratio	
G'=2265 Pa	E=6795 Pa
10% PEG vs gel at 1:0 ratio	
G'=10020 Pa	E=30060 Pa

4.5. Swelling measurements and mesh size calculation

Hydrogels are able to absorb large amounts of water and swell, which greatly affects their mechanical properties. Swelling was examined in respect to three different parameters: 1) PEG concentration, 2) the 4arm-PEG:2armPEG ratio (from 1:0 to 1:8); and 3) chemistry (vinyl sulfones versus maleimides). Swelling ratio (Q) was expressed as Q=Vs/V, where Vs is the volume of gels in the equilibrium-swollen state and V is the initial gel volume after formation.

For all the gels examined, the swelling was higher than 100%, meaning that gels took up water after gel formation, increasing their volume (Graph 4.9).

The overall tendency observed was that swelling increases with the weight percentage of PEG in the gel, which would be expected for ideal networks since there is more material in the same volume. In an ideal network, with only chemical cross-links

and no defects, the swelling ratio would have doubled from 5% to 10% gels. However, we always observed increases of a smaller extent between these two concentrations, presumably because the actual network structure in our gels is not ideal.

An exception to the trend of increase in swelling with concentration was observed for the lowest concentration studied (2% PEG maleimide gel). The increased swelling compared to the 3% gels can be explained by defects of the network that are expected due to the lower concentration of reactive groups. The very low weight percentage probably increases the probability that complementary reactive groups do not encounter each other to form covalent bonds.

The change of the ratio from 1:0 to 1:8 led to an increase in swelling of more than two times for PEG vs gels and about 20-30% for PEG maleimide gels.

The change of chemistry (vinyl sulfones versus maleimides) had different effect on 1:0 ratio gels and 1:8 ratio gels. For 1:0 gels it led to increase of the swelling for 15-20%. However, for 1:8 ratio gels this chemistry change led to the opposite: PEG vs gels swell 80-100% more than PEG maleimide gels at the same weight percentage.

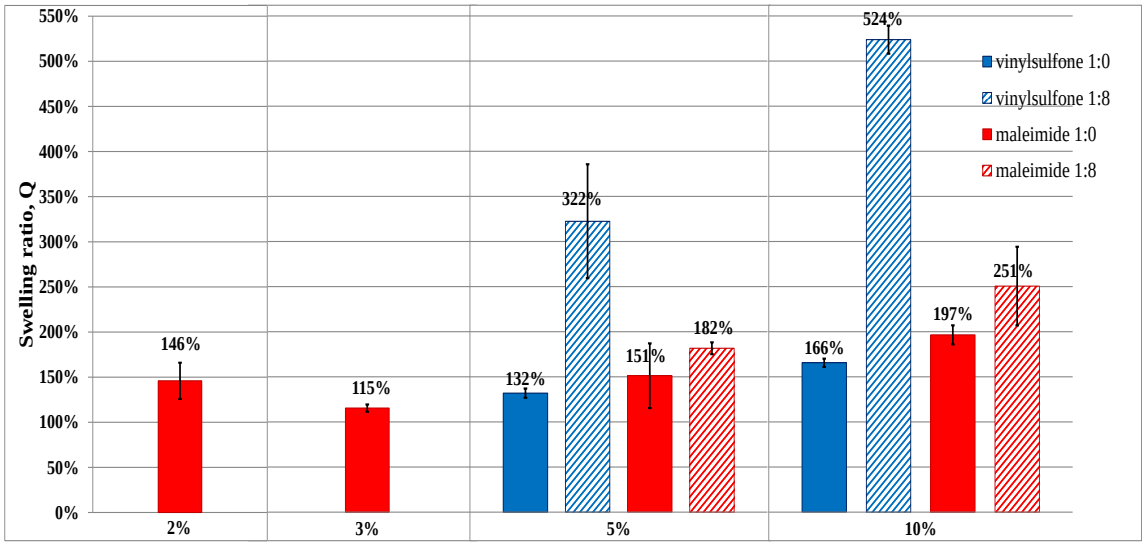

Graph 4.9. Swelling ratio of PEG vs and PEG maleimide hydrogels: 1:0 ratio is shown with the solid bars and 1:8 ratio is shown with the patterned bars; n=3. Error bars in the graph represent the standard deviation.

Based on established theoretical models described in section 2.2.3, we calculated the mesh sizes of different gels from swelling measurements (Graph 4.10). We observed that the mesh size of gels increases with a decrease in the weight percentage of PEG. For PEG vs gels at 1:0 ratio the mesh size lays within the range 16-20 nm. When changing the ratio from 1:0 to 1:8 at the same weight percentage the mesh size increases approximately two times (36-40 nm).

When changing the chemistry of the end-functional groups from vinyl sulfones to maleimides, the mesh size was essentially the same (about 1 nm difference) for the 1:0 ratio.

The change in ratio for maleimide gels (1:0 to 1:8) led only to a slight increase of the mesh size (1-2 nm), which is very different from the vs gels' behavior.

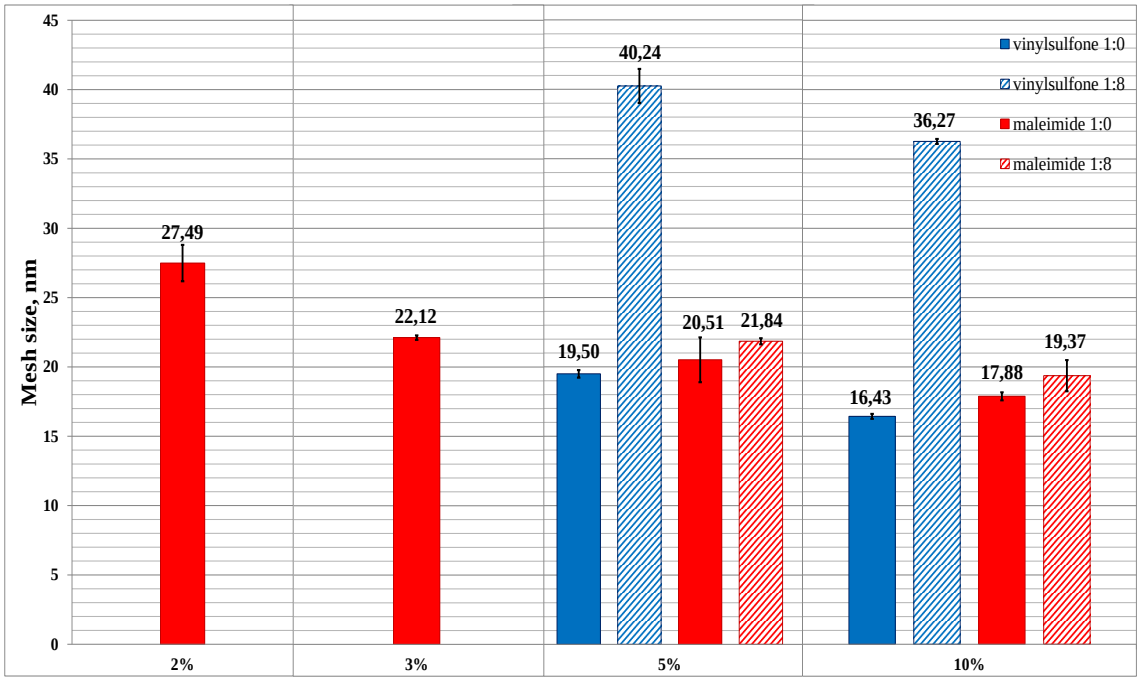

Graph 4.10. Calculated mesh sizes for different hydrogel formulations: 1:0 ratio is shown with the solid bars and 1:8 ratio is shown with the patterned bars, n=3. Error bars in the graph represent the standard deviation.

4.6. Beads encapsulation

The pore size calculated above (section 4.4.) is only a theoretical estimation of the actual pore size, assuming that the hydrogel network is homogeneous. An estimation of the actual pore size was performed by incorporating carboxylated beads of different sizes into the gels and observing their movement under the microscope. Encapsulated beads appeared immobile (Figure 4.1.) when performing a time lapse imaging for 3-5 minutes. The mobility of beads in the gels was checked in both non-swollen and swollen states. Moreover, the mobility of the beads was checked at different planes of the gels and appeared to be the same.

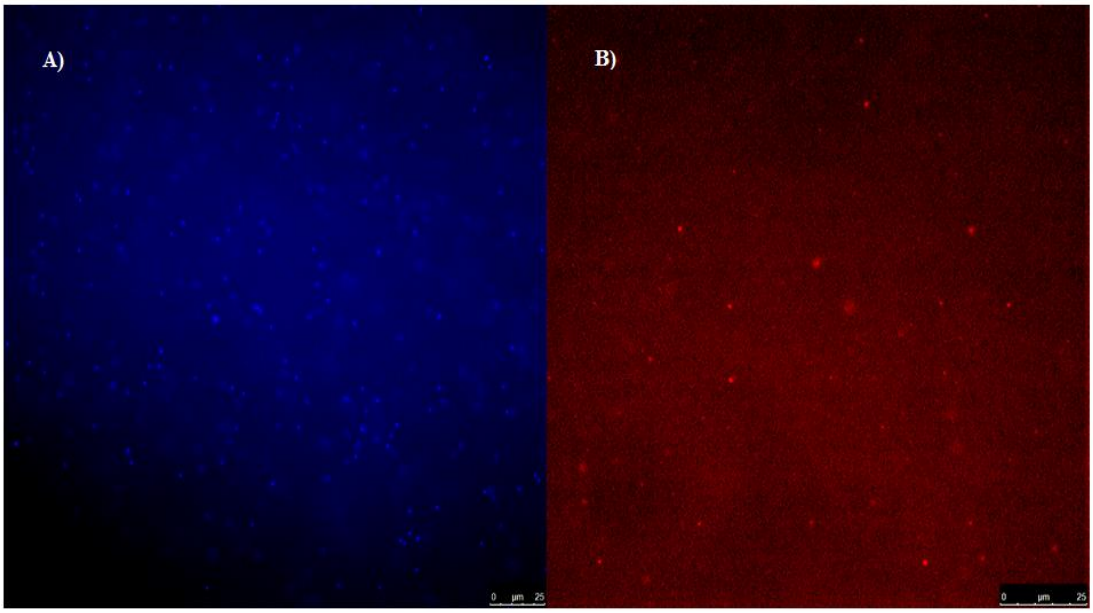

Figure 4.1. Frames from the time-lapse imaging of the immobilized carboxylated beads: A) 100 nm; B) 28 nm.

4.7. Dextran diffusion

We next decided to study the diffusion of encapsulated macromolecules (dextran) in the gels. The fluorescence intensity of encapsulated labeled dextran diffusing out of hydrogels was measured at different time points (Graph 4.11). It can be seen that the level of intensities for any of the dextran samples is significantly higher than for the control. Therefore, we can say that dextran is diffusing out from the gels. Moreover, the highest diffusion occurs almost immediately after the beginning of the experiment and does not change too drastically later. However, we cannot say at this point, if all the dextran diffused from the gels (and equilibrium was established) or only dextran that was very close to the surface diffused out while the majority of encapsulated dextran remained inside the gels.

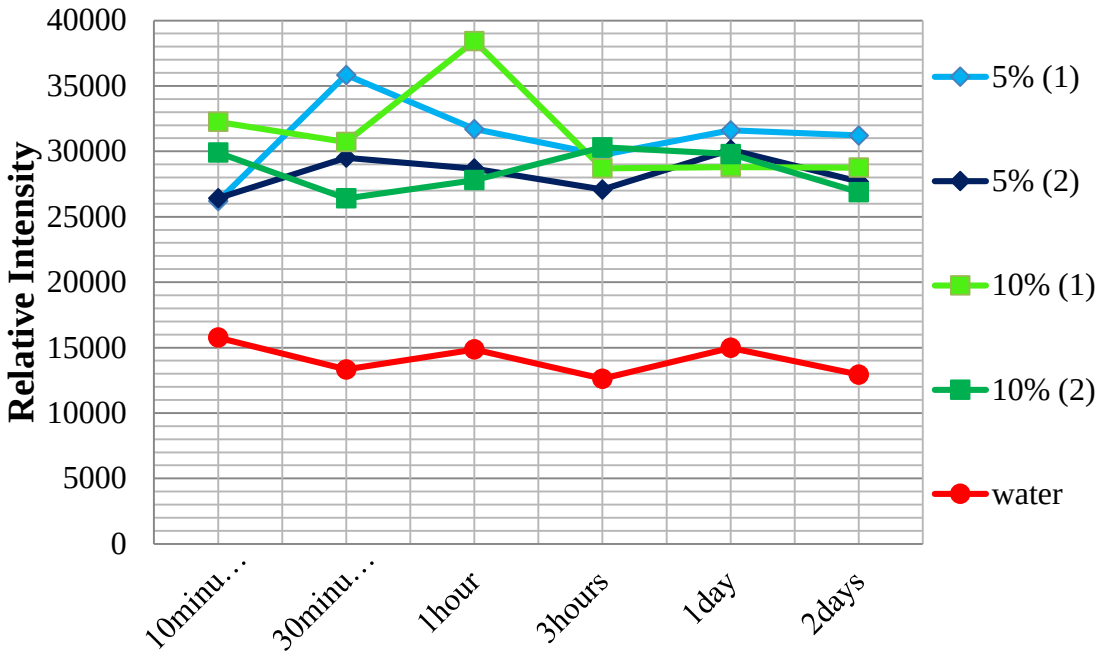

Graph 4.11. Diffusion of dextran out from the 5% and 10% hydrogels at 1:0 4arm-PEG:2arm-PEG ratio.

4.8. AFM

The Young's modulus of PEG vs hydrogels was measured as a function of: 1) PEG concentration, and 2) the 4arm-PEG:2armPEG ratio (from 1:0 to 1:8).

A significant increase in the Young's modulus (Graph 4.12) was observed when the PEG precursor concentration increased from 5% to 10% at the 1:0 ratio: 10% gels are almost 9 times stiffer than 5% ones. Moreover, the 10% gels at 1:0 ratio are more than 3 times stiffer than 10% gels at 1:8 ratio, which reflects the difference in the hydrogels microstructure as was expected based on our swelling measurements and mesh size calculations.

Attempts to measure gels from other formulations were not successful. The 5% gels at 1:8 did not form reproducibly as mentioned above (Section 4.2) and, therefore, we could not obtain reproducible data. In some cases where gels formed, the values of Young's modulus obtained were <1 kPa. Such values indicate very soft gels that are also very challenging to measure by AFM.

Concerning the PEG maleimide gels, the very rapid gelation made it impossible to prepare homogeneous gels for AFM.

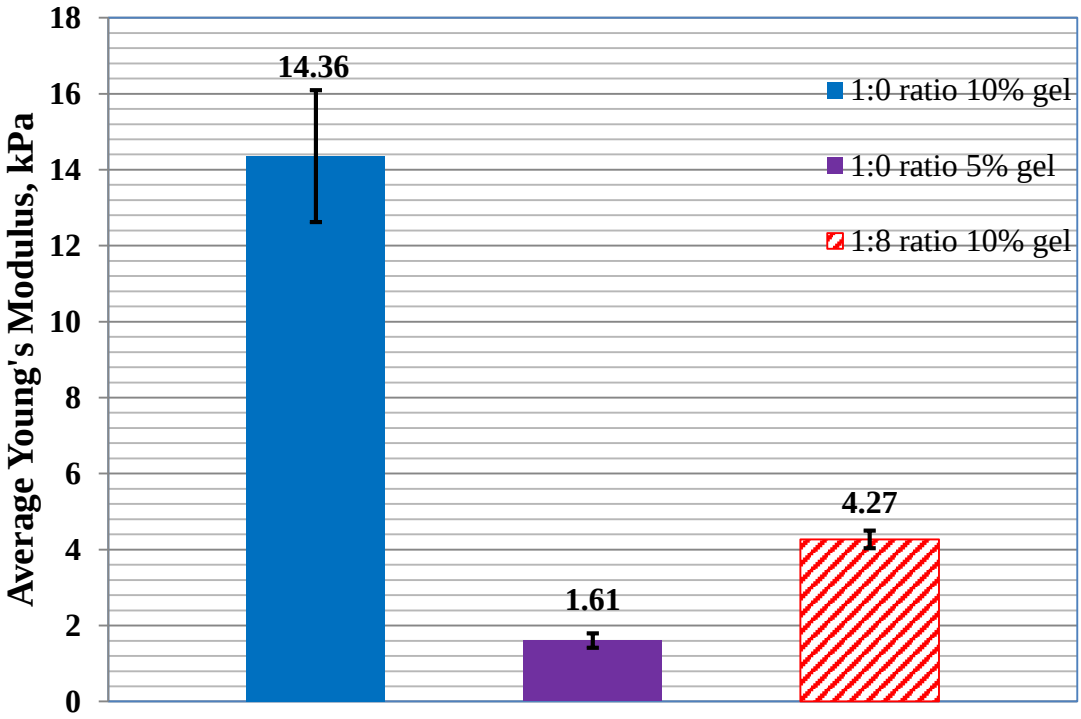

Graph 4.12. Young's modulus obtained from the AFM measurements; n=2, 3 positions each. Error bars in the graph represent the standard deviation. Hydrogels are in swollen state.

4.9. Cell viability

The modifications that were performed in the first part on this thesis were aiming to develop a PEG hydrogel suitable for cell encapsulation.

At first, LS174T cell encapsulation was attempted in 4arm-PEG 20k vs with DTT hydrogels at different concentrations (10%, 5%). Several hours after encapsulation, live cell microscopy revealed that in all cases cells were immobile and intracellular motion absent. We therefore concluded that cells were dead.

First, we examined whether the pH of our precursors was not responsible for killing the cells. The pH was found to be within 7-7.5, and therefore it is most likely not the cause of cell death.

The next hypothesis was that one of the precursors is toxic to the cells: either the vs or thiols are killing the cells while cross-linking reaction is still in process. To check this hypothesis, a live/dead viability assay was performed for cells seeded on a 96-well plate separately for different concentrations of PEG and for DTT (two wells for each concentration). The cells were checked using the DeltaVision inverted microscope at 10x magnification using FITC (467-498/ 513–556) and TRITC filters (532-554/ 570-613). However, it appeared that even at highest concentrations (1000 µg/ml for PEG and 500 µg/ml for DTT) the precursors do not kill the cells.

The following hypothesis was that even though the precursors are not killing the cells the reaction itself does. Several things were tried to check it. First, the time of cells addition to the precursor formulation was changed to observe reacting groups were toxic to the cells. However, even when increasing the time from 0 minutes to 15 minutes (the time to gelation is about 20 minutes) cells were still dead. Second, the ratio of vinyl sulfones to thiols was changed to see which of them has an effect on the cell viability. For 5% gels the vs:thiols ratio was changed from 1:1 to 1:0.9, 1:1.1 or 1:1.2. However, several hours after encapsulation in all of these cases the cells were immobile and intracellular motion was absent, and therefore cells were assumed dead. Nonetheless, the gels were left for several days to observe whether the spheroids are forming or not and to make sure that the cells were dead.

Finally, we decided to switch the cross-linker from DTT to cMMP peptide. This affects the chemistry since cMMP is cleavable by the metalloproteinases secreted by cells. Moreover, it largely affects the gelation range of the hydrogels: 4arm-PEG 20k vs gels with DTT do not form below 5% while gels with cMMP peptide are reproducibly forming even at 2%. For this type of gels a fraction of the cells survived the encapsulation process.

4.10. Cells encapsulation (growth)

LS174T cells tend to aggregate with each other. Therefore, when we refer in this study to the cell encapsulation, we mean both single encapsulated cells and encapsulated aggregates (of different size but about 2-10 cells each). In our experiments the majority of cells were aggregating and only few cells were single.

In this part of the project the LS174T cells were successfully encapsulated in 3D in 2% PEG hydrogel cross-linked with the cMMP peptide. The viability was improved by changing the ratio vs:thiols from 1:1 to 1:1.05 and 1:1.1. In our experiments at 1:1.1 vs:thiols ratio there were more alive cells directly after the encapsulation. Within the following week after the encapsulation the cell growth into spheroids was observed (Figure 4.2.). For 1:1.1 vs:thiols ratio the amount of spheroids growing was higher than for 1:1.05 ratio. However, only few of the cell aggregates, which were alive right after the encapsulation, grew into the spheroids: in two 10 µl hydrogels there were only 3 spheroids observed. In the future the volume of the gel could be increased to increase the amount of spheroids.

Furthermore, when checking the gels at different planes it was seen that cells were distributed throughout the whole gel, even though some sedimented to the bottom and attached to the glass substrate.

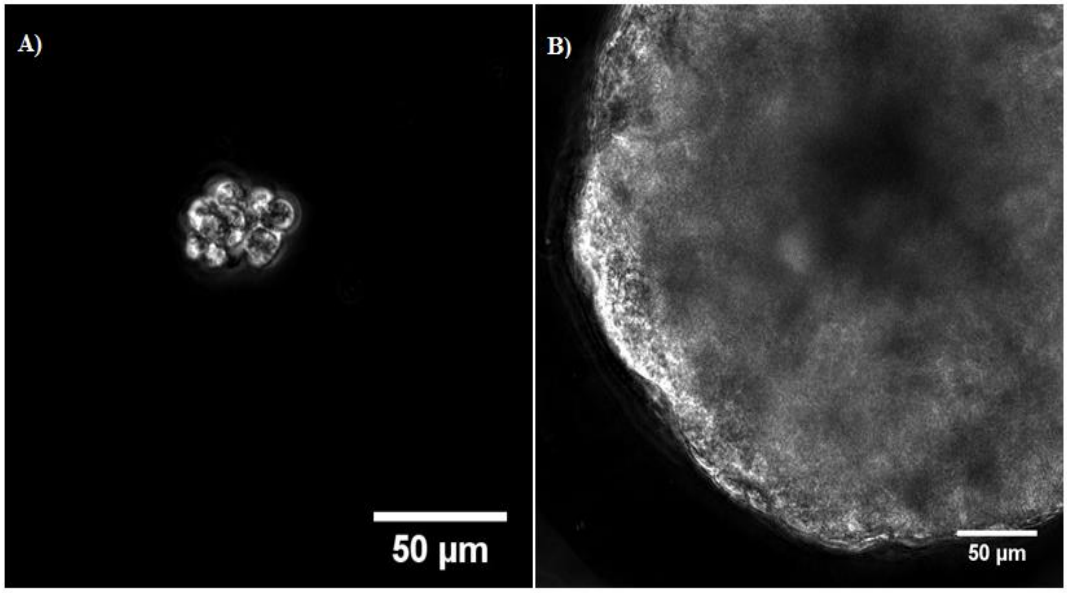

Figure 4.2. Example images of the LS174T tumor spheroid growth in PEG vs hydrogel: A) cell aggregate on day 1; B) spheroid on day 12.

5. Discussion

5.1. Hydrogel formation and structure

The initial objective of this project was to develop and evaluate a PEG hydrogel platform with controllable mechanical properties that would allow encapsulation and proliferation of live cells in a more physiological 3D setting. PEG hydrogels with controlled mechanical properties were prepared and their mechanical properties were evaluated. The manipulations needed to control the mechanical properties of these gels were rather simple: 1) change of the PEG concentration, 2) change of 4arm-PEG:2arm-PEG ratio. The mechanical properties that we controlled were stiffness and microstructural properties (pore size). Moreover, it is important to observe gelation kinetics since sometimes the gelation is either too slow or too fast, which may be inconvenient for certain experiments and should be chosen according to them. In this study the gelation range of a variety of formulations was obtained in the preliminary studies. Then gelation kinetics depending on the change of the PEG concentration was observed using oscillatory rheology. For all of the tested gels the storage modulus is increasing almost logarithmically over time. Therefore, relative increase in the storage modulus decreases with time and, as was observed, strongly depends on the concentration of PEG in the gel (Graphs 4.4 and 4.5).

During preliminary experiments, a problem with reproducibility of gel formation was revealed. To ensure the reproducibility, minimize the weighing errors and dilution effects the lyophilized aliquots were prepared from the precursors when possible. However, aliquoting appeared not to work for DTT and PEG maleimide. In case of DTT, it appeared to be volatile and was disappearing during the freeze-drying. In case of PEG maleimide, addition of PBS to the aliquoted PEG led to gelation. This could probably happen due to the spontaneous polymerization that occurred while aliquoting; however, no information about the cause of it was found in the literature.

PEG vs hydrogels were successfully prepared and their mechanical properties were tested using AFM indentation testing and oscillatory rheology. The higher Young's modulus for higher percentage gels indicates that there are more cross-links in the network which is consistent with the fact that there is more material in the same volume. We assumed that this could, possibly, be due to the higher probability of the vs groups to meet and react with thiols.

There is a large difference between the Young's moduli values obtained by AFM and by oscillatory rheology (2-fold for 10% gel and 4-fold for 5% gel). This can be explained by the fact that by AFM the Young's modulus was measured for gels in the swollen state while by rheology in the non-swollen.

According to the literature [31] the swelling ratio is linked to elastic modulus: the higher the swelling ratio (and consequently the bigger the pore size) the lower is the

elastic modulus. Therefore, the swelling data could be correlated with the AFM data, since the latter is obtained in the swollen state.

Nonetheless, the gelation range limits the further decrease of Young's modulus by changing the concentration of PEG in the precursor solution or changing the 4arm-PEG:2arm-PEG ratio.

The gelation range could be broadened by the change of the end-functional group's chemistry. Results of the experiments with PEG maleimide show that its reaction kinetics compared to that of PEG vs is dramatically faster which is consistent with previous studies. [36, 37]

Our data on the swelling/pore size suggests that the chemistry change from PEG vs to PEG maleimide would also have an effect on the mechanical properties, although, it was not proven by AFM or oscillatory rheology. An attempt to perform AFM for PEG maleimide gels was made; however, this was not possible due to the instantaneous gelation and, therefore, high inhomogeneity of the gels due to limited mixing.

At higher pH there are more thiolate anions in the solution that increases the rate of Michael-addition reaction. Therefore the problems associated with the very fast gelation could be possibly addressed by decreasing the pH to slightly acidic (6-7) and, therefore, decreasing the amount of thiolate anions. [37, 38]

Another possible way to deal with the instantaneous gelation would be the preparation of the long 2arm-PEG maleimide chains with DTT prior to the crosslinking with 4arm-PEG maleimide. This experiment was successfully performed and the gelation time was increased for low concentrations (3%). Moreover, the effect of the reaction time between 2arm-PEG and DTT prior to the cross-linking was observed. Due to time limitations of this project, it was not possible to reveal if there is a significant difference in mechanical properties of these gels, however, this would be interesting to study in the future.

One of the hypotheses of this study was that the controlled changes, which we performed on our hydrogel platform, affect the pore size. Our intension was to get large pore sizes (initial idea was to obtain pore size in the order of 100 nm). The hypothesis was that the increase of pore size would improve the diffusion of essential molecules (e.g. nutrients, growth factors) through the gels as well as make it easier for encapsulated cells to grow and migrate through these bigger pores. In overall, PEG hydrogels are dense networks of macromolecular chains and their porosity is significantly lower compared to the pore size of, for example, collagen type 1 which has pores of 1-10 μm depending on the concentration [12], or fibrin with the pore size of a 0.1-1 μm range. In this project the range of the pore sizes obtained was within 20 to 40 nm. In previous studies the pore size obtained for similar gels was stated to be about 25 nm. [12] Therefore, in this study we managed to significantly increase the pore size by incorporating the linear PEG between the cross-links. The possible further change of the 4arm-PEG:2arm-PEG ratio to 1:16 would potentially lead to the increase up to 50 nm (the value is calculated based on the schematic similar to the one in Figure 2.6 in section 2.2.3.). However, the gelation range for gels of 1:16 or any other ratio needs to be ex-

amined, since this change of 4arm-PEG:2arm-PEG ratio may have a large influence on gelation. Moreover, one should be careful when talking about the PEG concentration since through out of this study we referred to the weight concentration of 4arm-PEG. However, when changing the 4arm-PEG:2arm-PEG ratio we also introduce the bifunctional PEG and, therefore, we change the actual concentration of PEG.

In general, mesh size calculation is only an estimation of the average pore size assuming that the polymer network is homogeneous. However, in reality the network is not ideal due to the molecular defects, such as unreacted groups and dangling chains or physical entanglements, which would respectively either increase or decrease the pore size. These defects may occur due to the propensity of the thiol groups to undergo disulfide bond formation or just due to physically too long distance between the groups to react with each other. [38] Quantification of free thiols after gel formation indicates that there remains a significant percentage of unreacted thiols, which in turn suggest that the network of our hydrogels is not fully cross-linked.

In this project, the actual pore size was evaluated via incorporating particles of different size into the gels. Particle movement inside the gels was observed under the microscope. For the encapsulated particles, we observed no movement inside the gels, which is proving that particles which are bigger than calculated pore sizes are indeed immobilized. Therefore, dextran diffusion experiment was performed to reveal the mobility of smaller particles (several nm) inside the gel. This experiment showed that there is a significant diffusion of the dextran outside the gels shortly after the beginning of the experiment and it does not change dramatically at the later time points. This can be due to the fact that the concentration of dextran becomes more or less even in the sample and in the “sink” and there is no more diffusion gradient. This could be easily checked by removing the solution from above the gels and adding fresh MilliQ water on top to create a new gradient if it is the case.

Unfortunately, due to time limitations of this project it was not possible to check the actual pore size more systematically and compare it to the calculated one. However, it would be possible by incorporating into the gels a bigger variety of particles of a different size and observing their diffusion to identify the size limits of the particles that can diffuse through the network.

5.2. Cell encapsulation

An important aim of this study was to encapsulate cells into the PEG hydrogel matrix. This encapsulation was successfully performed for the LS174T cell line in 2% PEG 20k vs gels with cMMP peptide, with the majority of the cells surviving the encapsulation. Moreover, some of the encapsulated cells were able to grow inside the artificial hydrogels into spheroids.

Problems with cell survival were evident during initial attempts of encapsulation. Several possible reasons were investigated and suggested that the main problem

were the structural properties of the material. This could be the problem with the concentration of PEG being too high, and consequently gels being too stiff. The other possibility could be the problem with the cross-linker.

Cells were encapsulated in 5% and 3% gels with cMMP as a cross-linker instead of DTT. However, all of the cells appeared to be dead. When the concentration was decreased down to 2%, some of the cells survived the encapsulation. Therefore, we suggest that in our case the concentration of PEG has big impact on the cell survival and growth. The optimum conditions were found for vs:thiol ratio slightly lower than unity, which could be due to disulfide bond formation during reaction. [37]

In the future, potential improvements could be implemented on cell encapsulation in order to improve long-term viability. It is hypothesized that the biggest survival problem was the diffusion of molecules through the gels. The diffusion could be improved by increasing the pore size. Another possible option would be to prepare even softer gels. The strategies studied in the first part of this project could be implemented in order to achieve these objectives. One more potential option would be simply decreasing the size of the gels so that there is less distance for the molecules to diffuse through

Given the preliminary results presented in this Master's thesis, we believe the PEG hydrogels presented here hold the potential to be used as 3-dimensional substrates for cell studies. We believe it would be interesting in the future to systematically study how tumor spheroids grow as a function of hydrogel structural and mechanical properties.

6. Conclusions

6.1. Hydrogel formation and structure

Elastic, polymeric PEG hydrogels as a potential platform for 3D *in vitro* cell studies were successfully developed in the framework of this project. PEG hydrogels were prepared by Michael-type addition reaction of unsaturated double bonds to thiols which is mild and cytocompatible and, therefore, is suitable for live cells studies.

Our results have shown that it is possible to controllably modify the hydrogels' network architecture by applying several changes, such as 1) change of PEG concentration, 2) change of the 4arm-PEG:2armPEG ratio (from 1:0 to 1:8); and 3) change of chemistry (vinyl sulfones versus maleimides). The modification of the network architecture affects in turn the mesh size and elastic properties of hydrogels.

The range of polymerization and gelation kinetics was determined in respect to the above mentioned changes. Moreover, elastic properties were determined depending on the PEG concentration and 4arm-PEG:2armPEG ratio change. Furthermore, the swelling study was performed and theoretical hydrogels' mesh sizes were calculated.

Fluorescent, nanoscale beads were encapsulated inside the hydrogels, and microscopy showed that the encapsulated beads were immobile and could not diffuse within the hydrogels.

6.2. Cell encapsulation

The results of our cell encapsulation studies have shown that it is possible to encapsulate live LS174T cells using the type of hydrogels developed and evaluated in this project.

The precursors were proven to be non-toxic to the cells after short incubation periods at concentrations comparable to the concentrations used for hydrogel formation.

Phase contrast microscopy has shown that a large fraction of cells are successfully surviving the encapsulation. However, only a large minority of these was able to grow into spheroids afterwards. Thus, there are problems with the proliferation of the cells.

Finally, we can conclude that PEG hydrogels developed and evaluated in this project have a potential in the 3D *in vitro* live cells studies. Nonetheless, some challenges have to be met in order to improve the reproducibility of experiments and increase the cell viability.

7. References

1. Frantz C., Stewart K.M., and Weaver V.M.. 2010. The extracellular matrix at a glance. Journal of Cell Science, 123, 4195-4200.

2. Lutolf M.P., Hubbell J.A.. 2005. Synthetic biomaterials as instructive extracellular microenvironments for morphogenesis in tissue engineering. Nature Biotechnology, 23, 47-55.

3. Loessner D. et al. 2010. Bioengineered 3D platform to explore cell-ECM interactions and drug resistance of epithelial ovarian cancer cells. Biomaterials, 31, 8494-8506.

4. Kamata H. et al. 2014. "Nonswellable" Hydrogel without mechanical hysteresis. Science, 343, 873-875.

5. Even-Ram S., Yamada K.M. 2005. Cell migration in 3D matrix. Current Opinion in Cell Biology, 17, 524–532.

6. Patterson J., Hubbell J.A.. 2010. Enhanced proteolytic degradation of molecularly engineered PEG hydrogels in response to MMP-1 and MMP-2. Biomaterials, 31, 7836-7845.

7. Pathak A., Kumar S.. 2011. Biophysical regulation of tumor cell invasion - moving beyond matrix. Integrative Biology.

8. Miller, J.S. et al. 2010. Bioactive hydrogels made from step-growth derived PEG–peptide macromers. Biomaterials, 31, 3736-3743.

9. Seliktar D.. 2012. Designing Cell-Compatible Hydrogels for Biomedical Applications. Science, 336, 1124-1128.

10. Cole A. DeForest, Brian D. Polizzotti and Kristi S. Anseth. 2009. Sequential click reactions for synthesizing and patterning three-dimensional cell microenvironments. Nature Materials, 8, 660-664.

11. Lin C.-C., Anseth K. S.. 2009. PEG Hydrogels for the Controlled Release of Biomolecules in Regenerative Medicine. Pharmaceutical Research, 26, 631-643.

12. Raeber, G. P., Lutolf, M. P, and Hubbell, J. A.. 2005. Molecularly Engineered PEG Hydrogels: A Novel Model System for Proteolytically Mediated Cell Migration. Biophysical Journal, 89(2), 1374–1388.

13. Johnson K.L.. 1985. Contact mechanics, Cambridge University Press, Cambridge, 84-95.

14. Compiled by Dwyer-Joyce R. S.. 1997. Tribological Design Data Part 3: Contact Mechanics. 1st Edition, University of Sheffield.

15. JPK Instruments Application Report, available online: http://usa.jpk.com/afm.230.us.html, accessed on 30.06.2014.

16. JPK Instruments Technical Report, available online: http://www.jpk.com/afm.230.en.html, accessed on 30.06.2014.

17. Weitz D., Wyss H., Larsen R.. 2007. Oscillatory Rheology: Measuring the Viscoelastic Behavior of Soft Materials. G.I.T. Laboratory Journal 3-4, 68-70, GIT VERLAG GmbH & Co. KG, Darmstadt. Accessed online: http://www.google.de/url?sa=t&rct=j&q=&esrc=s&source=web&cd=1&ved=0CCsQFjAA&url=http%3A%2F%2Fwww.mate.tue.nl%2F~wyss%2Ffiles%2FWyss_GIT_Lab_J_2007.pdf&ei=ZFAwU7jxEeXOyAPN_4CwBg&usg=AFQjCNEjf9jtwoQS7m51UleZE_62hc4Zjw&sig2=xZdj7k6BlO6uMhyO7d8JnQ&bvm=bv.62922401,d.bGQ on 30.06.2014.

18. Kloxin A.M., Kloxin C.J., Bowman C.N., and Anseth K.S.. 2010. Mechanical Properties of Cellularly Responsive Hydrogels and Their Experimental Determination. Advanced Materials, 22, 3484–3494.

19. Canal, T., N. A. Peppas. 1989. Correlation between mesh size and equilibrium degree of swelling of polymeric networks. Journal of Biomedical Materials Research, Vol. 23, 1183–1193.

20. Vanderhooft J. L. et al. 2009. Rheological Properties of Cross-Linked Hyaluronan–Gelatin Hydrogels for Tissue Engineering, 9-1, 20–28.

21. Matsunaga T. et al. 2009. Structure Characterization of Tetra-PEG Gel by Small-Angle Neutron Scattering. Macromolecules, 42, 1344-1351.

22. Ertel A. et al. 2006. Pathway-specific differences between tumor cell lines and normal and tumor tissue cells. Molecular Cancer, 5:55.

23. The Culture Collections of Public Health England, available online: http://www.phe-culturecollec-

tions.org.uk/products/celllines/generalcell/detail.jsp?refId=87060401&collection=ecacc_gc, accessed on 30.06.2014.

24. Narayanan H. et al. 2010. *In silico* estimates of the free energy rates in growing tumor spheroids. Journal of physics: Condensed Matter 22, 194122

25. Unpublished: Mills K.L. et al, Elasticity and shape of prevascular solid tumors.

26. LS174T cell line characteristics, available online at: http://www.lgcstandards-atcc.org/products/all/CL-188.aspx?geo_country=de#characteristics, accessed on 30.06.2014.

27. JenKem Technology PEG Products Catalog 2013. Accessed online: http://www.jenkemusa.com/Pages/PEGProducts.aspx on 30.06.2014.

28. Product Specification. Sigma-Aldrich. Accessed online: http://www.sigmaaldrich.com/catalog/product/sigma/d9779?lang=de&region=DE on 30.06.2014.

29. Ellman's Reagent Product Instructions. Thermo Scientific. Available online: http://www.piercenet.com/pisearch/?prodnum=22582 Accessed on 30.06.2014.

30. Sudholter E., De Smet L., Mescher M. and Uliien D.. 2011. Organic Surface Modification of Silicon Nanowire-Based Sensor Devices, Nanowires - Implementations and Applications. Dr. Abbass Hashim (Ed.), ISBN: 978-953-307-318-7, InTech, Available from: http://www.intechopen.com/books/nanowires-implementations-and-applications/organic-surface-modification-of-silicon-nanowire-based-sensor-devices.

31. Lutolf, M. P., Hubbell, J. A.. 2003. Synthesis and Physicochemical Characterization of End-Linked Poly(ethylene glycol)-co-peptide Hydrogels Formed by Michael-Type Addition. Biomacromolecules, 4, 713-722.

32. Patterson, J., Hubbell, J.A.. 2010. Enhanced proteolytic degradation of molecularly engineered PEG hydrogels in response to MMP1 and MMP2. Biomaterials, 31, 7836-7845.

33. Product Specification. Sigma-Aldrich. Accessed online: http://www.sigmaaldrich.com/catalog/product/aldrich/m9768?lang=de&region=DE on 30.06.2014.

34. Product Specification. Sigma-Aldrich. Accessed online: http://www.sigmaaldrich.com/catalog/product/sial/a3648?lang=de&region=DE on 30.06.2014.

35. Product Specification. Sigma-Aldrich. Accessed online: http://www.sigmaaldrich.com/catalog/product/sigma/e6511?lang=de&region=DE on 30.06.2014.

36. Phelps E.A. et al. 2012. Maleimide cross-linked bioactive PEG hydrogel exhibits improved reaction kinetics and cross-linking for cell encapsulation and in-situ delivery. Advanced Materials, Volume 24(1), 64–2.

37. Canalle L.A. et al. 2010. Polypeptide–polymer bioconjugates. Chemical Society Reviews, 39, 329–353.

38. Mather B.D.. 2006. Michael addition reactions in macromolecular design for emerging technologies. Progress in Polymer Science, 31, 487–531.

39. Nemir. S., West, J.L.. 2010. Synthetic Materials in the Study of Cell Response to Substrate Rigidity. Annals of Biomedical Engineering, 38, 2-20.

40. Tang X. et al. 2010. Mechanical Force Affects Expression of an In Vitro Metastasis-Like Phenotype in HCT-8 Cells. Biophysical Journal, 99, 2460–2469.